International Journal of Nanomedicine

Dovepress
open access to scientific and medical research

Open Access Full Text Article

REVIEW

Antibacterial Pathways in Transition Metal-Based Nanocomposites: A Mechanistic Overview

Chinmaya Mutalik[1,2], I-Hsin Lin[3], Dyah Ika Krisnawati[4], Siti Khaerunnisa[5], Muhamad Khafid[6], Widodo[7], Yu-Cheng Hsiao[1,8–10], Tsung-Rong Kuo[1,2]

[1]International Ph.D. Program in Biomedical Engineering, College of Biomedical Engineering, Taipei Medical University, Taipei, Taiwan; [2]Graduate Institute of Nanomedicine and Medical Engineering, College of Biomedical Engineering, Taipei Medical University, Taipei, Taiwan; [3]School of Biomedical Engineering, College of Biomedical Engineering, Taipei Medical University, Taipei, Taiwan; [4]Dharma Husada Nursing Academy, Kediri, Indonesia; [5]Department of Physiology and Medical Biochemistry, Faculty of Medicine, Universitas Airlangga, Surabaya, Indonesia; [6]Department of Nursing, Faculty of Nursing and Midwifery, Universitas Nahdlatul Ulama Surabaya, East Java, Indonesia; [7]College of Information System, Universitas Nusantara PGRI, Kediri, Indonesia; [8]Graduate Institute of Biomedical Optomechatronics, College of Biomedical Engineering, Taipei Medical University, Taipei, Taiwan; [9]Cell Physiology and Molecular Image Research Center, Wan Fang Hospital, Taipei Medical University, Taipei, Taiwan; [10]Stanford Byers Center for Biodesign, Stanford University, Stanford, CA, USA

Correspondence: Yu-Cheng Hsiao; Tsung-Rong Kuo, Tel +886-2-66382736 ext. 1359; +886-2-27361661 ext. 7706, Email ychsiao@tmu.edu.tw; trkuo@tmu.edu.tw

Abstract: Across the planet, outbreaks of bacterial illnesses pose major health risks and raise concerns. Photodynamic, photothermal, and metal ion release effects of transition metal-based nanocomposites (TMNs) were recently shown to be highly effective in reducing bacterial resistance and upsurges in outbreaks. Surface plasmonic resonance, photonics, crystal structures, and optical properties of TMNs have been used to regulate metal ion release, produce oxidative stress, and generate heat for bactericidal applications. The superior properties of TMNs provide a chance to investigate and improve their antimicrobial actions, perhaps leading to therapeutic interventions. In this review, we discuss three alternative antibacterial strategies based on TMNs of photodynamic therapy, photothermal therapy, and metal ion release and their mechanistic actions. The scientific community has made significant efforts to address the safety, effectiveness, toxicity, and biocompatibility of these metallic nanostructures; significant achievements and trends have been highlighted in this review. The combination of therapies together has borne significant results to counter antimicrobial resistance (4-log reduction). These three antimicrobial pathways are separated into subcategories based on recent successes, highlighting potential needs and challenges in medical, environmental, and allied industries.

Keywords: transition metals, nanocomposites, photodynamic, photothermal, metal ion release, antibacterial mechanisms

Introduction

Contagious infections caused by bacteria, fungi, and viruses continue to be major global health concerns, necessitating the regular development of new antimicrobial materials.[1] Antibiotic-resistant bacteria cause over 2 million infections and over 23,000 deaths each year, according to the World Health Organization (WHO).[2] These figures have prompted researchers to look into alternate antimicrobial drugs that can efficiently inhibit pathogenic germs while causing no harm to the host organism.[3] As a tool, nanotechnology has been rapidly integrated into various spheres of life, including the health sector.[4] Nanotechnology has a wide range of applications in the health industry, ranging from diagnostics to therapeutics. One of the most difficult therapeutic stresses on a global scale is the treatment of bacterial infections. Indeed, long-term use and misuse of antibiotics via several channels such as livestock, food, and water have resulted in antibiotic resistance, which poses great risks to public health.[5–7] Photodynamic therapy (PDT), photothermal therapy (PTT), and metal ion release incorporating transition metal dichalcogenides (TMDCs), transition metal chalcogenides (TMCs), transition metals (TMs), and transition metal oxides (TMOs) are all significant approaches for a variety of biological applications. Multiple TMOs and sulfides, and their organic and inorganic nanocomposites have been studied in clinical trials for treating chronic and acute diseases, cancer, and health problems caused by microorganisms.[8–13]

Received: 3 October 2022
Accepted: 22 December 2022
Published: 30 December 2022

Graphical Abstract

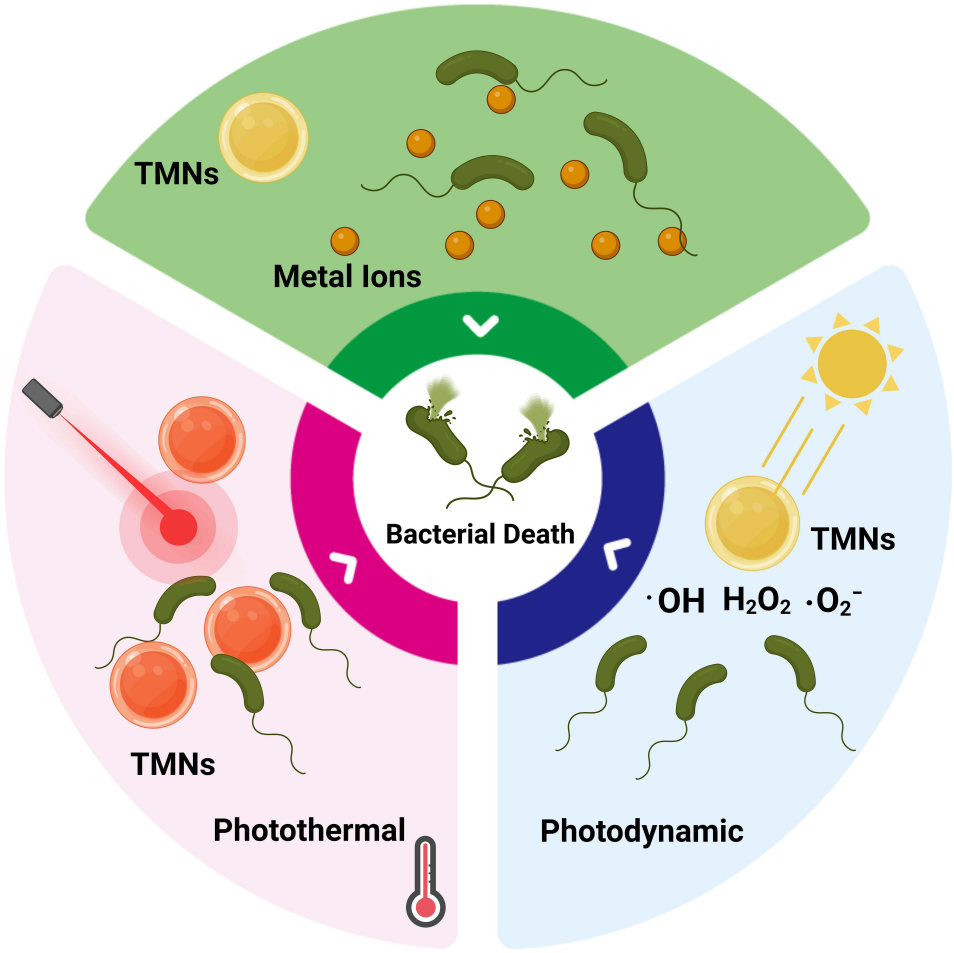

Moreover, two-dimensional (2D) TMDCs, TMCs, TMs, and TMOs are a new family of materials with features that make them appealing for the fundamental study of novel physical phenomena as well as applications spanning nanomedicine, nanoelectronics, and nanophotonics for nanosensing and actuation.[14] TMDCs, TMCs, TMs, and TMOs are a diverse class of 2D layered materials that are both technically and industrially significant. Because of their unusual structural properties and intriguing applications in fields of health, environment, optoelectronics, electronics, mechanics, optics, catalysts, energy-storage, thermal, and superconductivity, these nanomaterials have garnered a lot of attention.[15–24] TMDCs are chemical compounds with the formula MX_2, where M is a TM element from groups IV~VII B (Mo, W, V, Nb, Ta, Ti, Zr, Hf, Tc, and Re) and X is a chalcogen element (S, Se, and Te). The X-M-X unit layer is made up of three atomic layers, with one central atom layer (M) sandwiched between two chalcogen atom (X) layers and other metal disulfides that are used in numerous bio-related applications. Further, chalcogenides have a complex fibrillar structure; for example, covellite (CuS) is arranged in alternative layers of Cu_2S_2 containing copper atoms in unique trigonal planar and tetrahedral coordination. TiO_2, CuO, ZnO, Fe_2O_3, and other TMOs, and their composites are photoactive semiconductors, are biologically active which is attributed to their structural and optical properties, and are frequently used for antibacterial and antifungal activity for *Escherichia coli* (*E. coli), Staphylococcus aureus* (*S. aureus*), *Rhizopus stolonifer, Rhizopus oryzae*, etc.[25–28] TMDCs are found in layered formations similar to graphite. Exfoliation causes the interlayers to stack due to weak van der Waals forces, resulting in the creation of monolayers or nanolayers from bulk materials.[29]

Furthermore, PDT and PTT in combination with diverse TMDCs, TMCs, TMOs, and their composites use light to initiate a chain of events that results in bacterial death. PDT makes use of photosensitizers or their precursors, which can absorb visible light and form reactive oxygen species (ROS) that are hazardous to cells due to oxidative stress. Metals, up-conversion nanoparticles (NPs), carbon-based nanomaterials such as 2D TMDC, TMC, TM, and TMO nanoforms, and their composite materials are used in PDT applications.[30–33] The ZnO-V_2O_5-WO_3, ZnO-Er_2O_3-Nd_2O_3@rGO, TiO_2-Y_2O_3-V_2O_5, and Fe_2O_3-PANI nanocomposites have shown increased activity in photocatalytic performance and antibacterial activity against *E. coli, Klebsiella pneumonia, Staphylococcus aureus, Proteus vulgaris*, and *Pseudomonas aeruginosa* bacteria.[34–38] PTT uses photothermal NPs, which absorb light and convert it to heat, resulting in hyperthermia, which kills cells. A near-infrared (NIR) laser is preferred as a light source for this therapy due to therapeutic benefits such as deeper tissue penetration, safety, and high absorption by photothermal agents (PTAs).[39,40] Furthermore, in a biological context, by losing electrons, metal atoms can quickly become positively charged ions, which can subsequently dissolve in biological fluids. Metal ions have a high affinity for electron-rich biomolecules such as DNA and proteins, with which they form complexes due to their electron shortage. Complex building structures result in protein inactivation, DNA damage, membrane disruption, and eventual bacterial mortality.[41–43] In this review, we discuss three approaches for combating bacteria utilizing 2D TMDC, TMC, TM, and TMO based-nanomaterials: PDT, PTT, and metal ion release. Following that, a quick overview of trends in new antibacterial medication approaches is offered.

Photodynamic Dynamic Antibacterial Therapy

Mechanistic Overview of Photodynamic Therapy

Light-actuated materials have been used for some time to treat infections, and for more than 100 years this has been called photodynamic therapy (PDT). PDT needs two components to be useful: light and a material or compound that can be sharpened by bright ultraviolet (UV) or apparent locales of the electromagnetic range of visible light illumination (Figure 1). Currently, photodynamic therapy is employed as an alternative therapy for the management of malignant disorders. It is based on the uptake of a photosensitizer molecule, which, when activated by light at a specific wavelength, combines with oxygen to produce oxidant species (radicals, singlet oxygen, and triplet species), which cause cell death in the target areas. It has been determined that PDT's cytotoxic effects result from the oxidation of a wide variety of biomolecules in cells, including nucleic acids, lipids, and proteins, which causes a serious modification in cell signaling cascades or in the regulation of gene expression.[44] The mechanism of PDT is described by two sorts of pathways: type I reaction involves electrons and holes transfer to generate radical and radical anion species and type 2 reaction goes through with energy transfer between oxygen and excited nanomaterials. The type I response system of nanomaterials under light illumination can produce ROS like hydroxyl radical (·OH), superoxide anion ($\cdot O_2^-$), and hydrogen peroxide and requires higher actuation energy. The type II component produces singlet oxygen ($^1O_2$), requires lower actuation energy, and is more promptly accessible. Some metallic nanostructures like TiO-WO_3-CeO_2, PANI-CeO_2-Fe_2O_3-NiO, rGO-ZnO-Ho_2O_3-Sm_2O_3, PANI-ZnO-Ho_2O_3-Sm_2O_3 nanocomposites and metal-organic frameworks have been widely

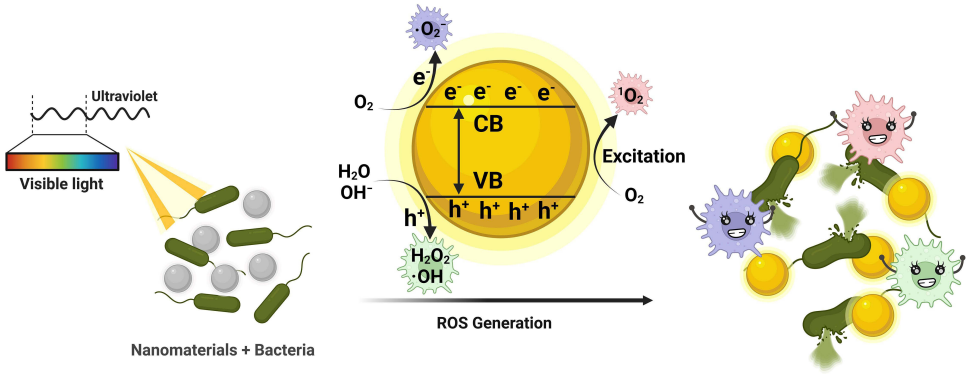

Figure 1 Schematic illustration of the photodynamic antibacterial pathway of nanomaterials.

used because of their unrivaled photocatalytic properties, minimal expense, the bandgap is substantially reduced when compared to their single metallic nanostructures, and compelling antibacterial properties.[45–47] NPs under notable light illumination are accepted as compelling photocatalysts and can create ROS for powerful antibacterial actions.[48–53]

Photodynamic Mechanisms of Transition Metals and Their Composites

In our recent study, we reported photodynamic action of CuS nanosheets (NSs) under simulated sunlight irradiation based on ROS and electron spin resonance (ESR) data, and a reaction mechanism for photocatalysis was postulated (Figure 2A).[54] CuS NSs and CuS NPs outperformed their counterparts in terms of photoactivity and antibacterial efficiency in creating ROS, such as ·OH and $\cdot O_2^-$ radicals. In addition, simulated light irradiation of CuS microspheres (MSs), CuS NSs, and CuS NPs produced photoelectrons and holes, which produced ROS such as ·OH and $\cdot O_2^-$ radicals. As a result, as previously stated, CuS undergoes photodegradation, which produces sulfur vacancies, copper ions, and carbon residues, resulting in the adsorption of ambient moisture (validated by UV-visible-NIR spectroscopy and ESR). Furthermore, the conduction mechanism in CuS NSs and CuS NPs is elicited by ambient oxygen under solar light illumination due to the presence of carbon and oxygen remnants. As a result, carbon and oxygen remnants in CuS NSs and CuS NPs allow the further formation of $\cdot O_2^-$ radicals by photocatalytic electron transport while also narrowing the gap between CuS NS and CuS NP valence bands (VBs) and conduction bands (CBs). CuS NSs and CuS NPs generate ·OH and $\cdot O_2^-$ radicals that permanently damage bacterial cell envelopes. Furthermore, *E. coli* growth curves of CuS NSs and CuSNPs were consistent with prior research on ROS generation and radical identification.[55–57]

The metallic phase of 1T-MoS_2 nanoflowers (NFs) and the semiconducting phase of 2H-MoS_2 NFs were discovered to be photoactive when exposed to visible light (at ca. 400~700 nm).[58] In this work, metallic 1T-MoS_2 NFs were shown to create more ROS than semiconducting 2H-MoS_2 NFs when exposed to light. The enhanced light-driven antibacterial activity of 1T-MoS_2 NFs over 2H-MoS_2 NFs can possibly be attributed to phase variations between the metallic and semiconducting phases. Previous research showed that metallic 1T-MoS_2 NFs emit photoelectrons when exposed to light via a photoelectronic effect. The mechanism of light-driven antibacterial action of 1T-MoS_2 NFs appears to be that when exposed to light, photoelectrons created by metallic 1T-MoS_2 NFs interact with oxygen to produce superoxide ($\cdot O_2^-$), as illustrated in Figure 2B. When exposed to light, semiconducting 2H-MoS_2 NFs create photoinduced electron-hole pairs. Photoinduced electron-hole pair recombination reduces the efficiency of ROS production in semiconducting 2H-MoS_2 NFs, resulting in a reduction in the light-driven antibacterial function. As a consequence, metallic 1T-MoS_2 NFs were shown to exhibit more light-driven antimicrobial properties than semiconducting 2H-MoS_2 NFs. Metallic 1T-MoS_2 NFs, with their excellent photoactivity and simple fabrication, might be a potential light-driven antimicrobial for advances in food security, water cleansing, and medical sterilization. The mechanism of highly light-driven antibacterial action of metallic 1T-MoS_2 NFs is that when exposed to light, metallic 1T-MoS_2 NFs create photoelectrons, which subsequently

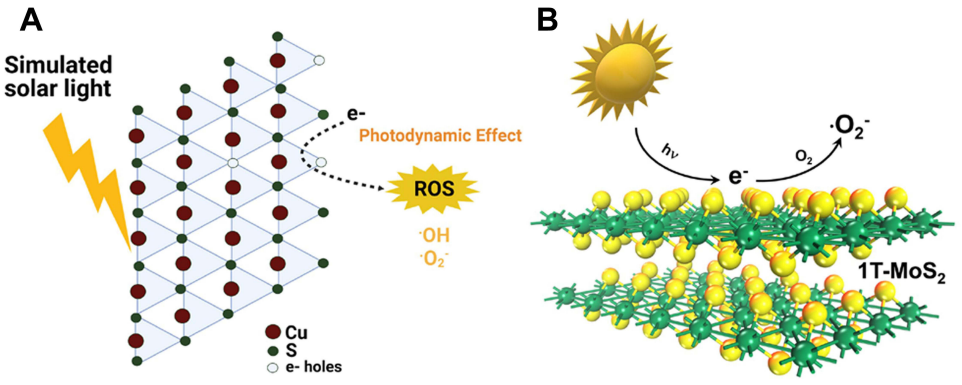

Figure 2 (**A**) Copper sulfide nanosheet photodynamic antibacterial pathway. Reprinted from *J. Colloid Interface Sci*; Volume: 607, Mutalik C, Okoro G, Krisnawati DI, et al. Copper sulfide with morphology-dependent photodynamic and photothermal antibacterial activities. 1825–1835, Copyright (2022), with permission from Elsevier.[54] (**B**) The production of photodynamic superoxide ($\cdot O_2^-$) by 1T-MoS_2 nanoflowers. Reprinted with permission from Mutalik C, Krisnawati, DI, Patil SB, et al. Phase-dependent MoS2 nanoflowers for light-driven antibacterial application. *ACS Sustain. Chem. Eng.* 2021;(9):7904–7912. Copyright (2021). American Chemical Society.[58]

combine with oxygen to produce superoxide, which causes bacterial death. When exposed to light, semiconducting 2H-MoS_2 NFs generate photoinduced electron-hole pairs, and the recombination of the photoinduced electrons and holes reduces the production of ROS, lowering light-driven antibacterial activity.[58–62]

In one of our recent studies, we noted that according to bacterial growth data, light-induced antibacterial activity increased in the sequence of FeS_2 NPs, TiO_2 NPs, and TiO_2/FeS_2 nanocomposites (NCs).[63] Moreover, the mechanism was explained using bandgaps of TiO_2 NPs and FeS_2 NPs in the UV-visible-NIR range of the electromagnetic spectrum estimated to be 3.2 and 0.95 eV, respectively, using a schematic representation (Figure 3).[64] Pairing TiO_2 NPs and FeS_2 NPs was found to increase the photoactivity. TiO_2/FeS_2 NCs were found to have greater light-induced antibacterial activity than TiO_2 NPs or FeS_2 NPs alone in that investigation. Figure 4A displays a schematic of the mechanism of light-induced antibacterial activity in TiO_2/FeS_2 NCs. When compared to a traditional hydrogen electrode, the CB and VB of TiO_2 NPs were 0.2 and 3 eV, respectively (normal hydrogen electrode (NHE)). As an outcome, TiO_2 NPs can absorb UV radiation and generate photoinduced electrons and holes, allowing ROS such as $\cdot O_2^-$ (0.16 eV) and ·OH (2.32 eV) to develop. For FeS_2 NPs, the CB and VB reached 0.5 and 0.45 eV, respectively. In TiO_2/FeS_2 NCs, FeS_2 NPs act as light harvesters, capturing visible to NIR radiation to generate photoinduced electrons and holes. Photoinduced electrons in the CB of FeS_2 NPs are transferred to the CB of TiO_2 NPs to increase ROS formation. Because of the broad range of

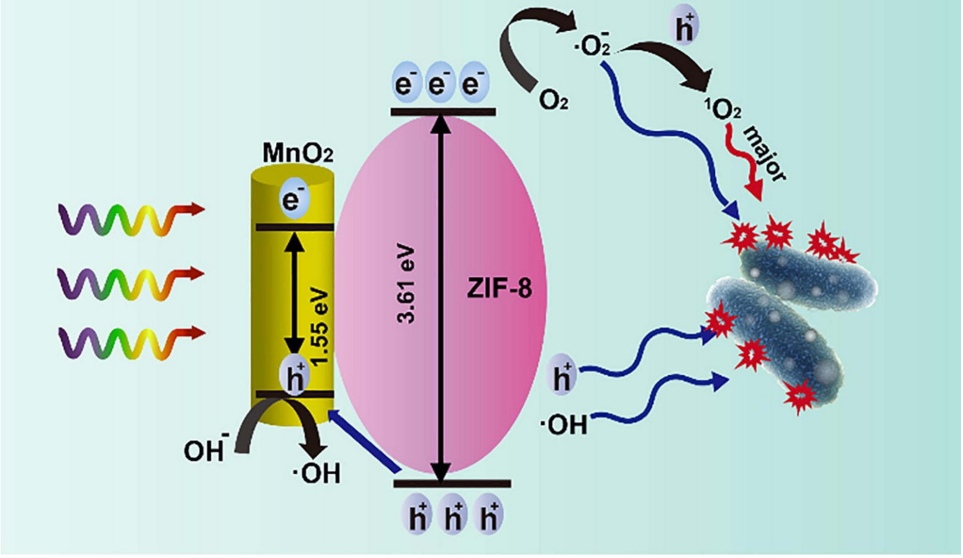

Figure 3 Photodynamic antibacterial pathway of MnO_2/zeolitic imidazole framework (ZIF)-8. Reprinted from *Chem. Eng. J*, Volume: 428. Liang Z, Wang H, Zhang K, et al. Oxygen-defective mno2/zif-8 nanorods with enhanced antibacterial activity under solar light. 131349, Copyright 2022, with permission from Elsevier.[64]

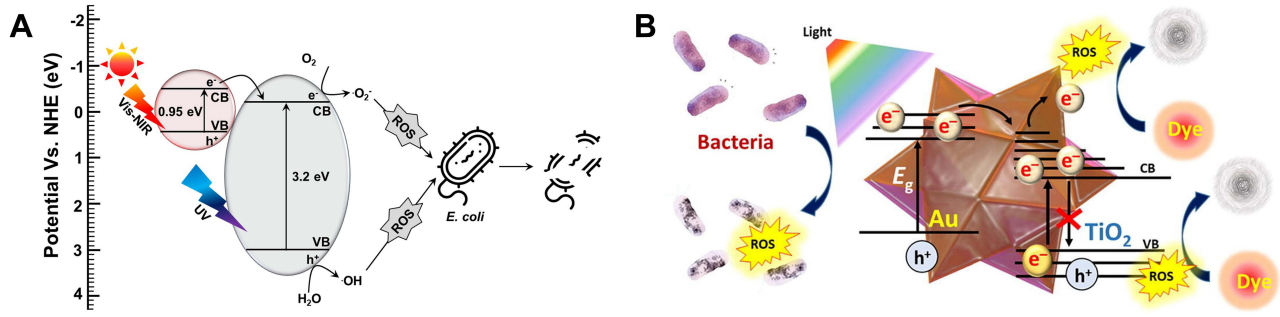

Figure 4 (**A**) Proposed photodynamic antibacterial pathway for TiO_2/FeS_2 nanocomposites (NCs). Reproduced with permission from Dove Medical Press. Mutalik C, Hsiao YC, Chang YH, et al. High UV-Vis-NIR light-induced antibacterial activity by heterostructured TiO_2-FeS_2 nanocomposites. *Int J Nanomedicine*. 2020;(15): 8911–8920.[63] (**B**) Photodynamic antibacterial pathway of TiOx-Au NCs) (50:1). Reprinted from *J. Colloid Interface Sci.* Volume: 598, Unnikrishnan B, Gultom IS, Tseng YT, Chang HT, Huang CC. Controlling morphology evolution of titanium oxide–gold nanourchin for photocatalytic degradation of dyes and photoinactivation of bacteria in the infected wound. 260–273, Copyright (2021), with permission from Elsevier.[69]

light absorption from UV to NIR, light harvesters of FeS_2 NPs increase the light-induced antibacterial activity of TiO_2 /FeS_2 NCs.[65–68]

In a recent example, authors preferred TiOx-gold (Au) NCs (50:1) because TiOx-Au NCs (50:1) have strong photocatalytic activity, and they were used for photocatalytic bacterial disinfection.[69] Using radiation from a xenon arc lamp, gram-negative (*E. coli*) and gram-positive methicillin-resistant *Staphylococcus aureus* (MRSA) bacteria were photocatalytically inactivated, and a schematic illustration of the antibacterial mechanism is shown in Figure 4B. The reason for P25 with lower antimicrobial activities is that pristine TiO_2 struggles with electron-hole pair coupling, which results in a lack of free radicals. High levels of ROS created during the optical excitation of TiOx-Au NCs cause oxidative stress in bacteria, resulting in cell death. Albeit without light irradiation, TiOx-Au NCs showed antibacterial activity against MRSA (the bacterial survival rate fell to 50%), which could have been due to physical interactions between the pointed end of urchin-like NPs and bacterial walls throughout the culture. The antibacterial impact was additionally aided by TiOx-Au NCs damaging bacterial cell membranes. According to reports, bacteria were killed by a physicomechanical breakdown of cell walls caused by the tiny spines on the surface of the NPs. MRSA and photocatalysts had a stronger interaction than that with *E. coli*, which could explain why they were removed in the dark. The antimicrobial activity of nanomaterials varies depending on the substance and bacterial strain, according to investigations. Without light irradiation, *E. coli* showed greater resistance to TiOx-Au NCs (50:1). Numerous catechin analogues were shown to exhibit antimicrobial properties against gram-positive bacteria by breaking down bacterial walls; therefore, it was believed that the thin coating of poly(catechin) over TiOx-Au NCs (50:1) was correlated with the bactericidal effect against MRSA. Furthermore, with light irradiation, TiOx-Au NCs showed strong green fluorescence, suggesting that a significant concentration of intracellular ROS had formed, causing bacterial death. The light-assisted creation of ROS was primarily responsible for the photocatalytic removal of dyes and the deactivation of bacteria and fungi. However, compared to *E. coli* and *Candida albicans*, the photocatalyst had greater effectiveness in neutralizing MRSA due to significant engagement among them.[69–74]

For the first time, MnO_2 was modified with zeolitic imidazole framework (ZIF)-8 to improve its photocatalytic bactericidal performance.[64] With simulated sun irradiation, MnO_2/ZIF-8 completely inactivated multidrug-resistant (MDR) *E. coli* at a low dose (3.24 g/mL). The primary reactive species for bacterial inactivation was discovered to be $^1O_2$, rather than the $\cdot O_2^-$ radical or ·OH radical. Thus, a likely mechanism of MnO_2/ZIF-8 with antibacterial action is as follows. ZIF-8 electrons (e^-) are stimulated from the VB to the CB by light irradiation, leaving holes in the VB. These photoinduced electrons then react with O_2 ($E(O_2/\text{radical } \cdot O_2^-) = 0.33$ V) adsorbed at the surface oxygen vacancies, resulting in the creation of $\cdot O_2$ radicals, which are then oxidized by holes into $^1O_2$. On the other hand, the holes at the ZIF-8 VB are pumped into the MnO_2 VB, inhibiting electron-hole pair recombination. OH^- ($E(OH^-/\text{radical } \cdot OH)$) might then react with the holes in the MnO_2 VB to create ·OH radicals. In Figure 3, mechanistic studies revealed that the bactericidal property of MnO_2/ZIF-8 over pure material was attributed to enhanced surface oxygen vacancy and hindered electron/hole recombination. The increased photocatalytic activity of the MnO_2/ZIF-8 hybrid structure compared to the pure material gave it superior bacterial inactivation efficiency. This research presented a novel form of a photocatalyst for antibacterial applications and may throw light on the development of low-cost MnO_2-based nanocomposites with photocatalytic bactericidal capacity for practical water disinfection treatment and other biological applications.[75–77]

A novel technique to fabricate Au/Ti_3C_2 photoactive membranes that can be employed as a superior interface photoactive material can produce efficient evaporation and antibacterial properties when exposed to solar light. The Au/Ti_3C_2 membrane has a unique 2D layer overlapping structure with a surface plasmon resonance (SPR) effect and outstanding solar light-to-heat conversion capabilities. When the inhibitor of furfuryl alcohol corresponding to $^1O_2$ was added to the bacterial inactivation process without the presence of scavengers, the inhibitory impact was most visible, showing that $^1O_2$ contributed the most to bacterial inactivation (Figure 5A). When inhibitors of $\cdot O^{2-}$, electron, and hole (p-BQ, $K_2Cr_2O_7$, and $Na_2C_2O_4$, respectively) were introduced, the bactericidal performance was inhibited and the degree of inhibition was comparable, showing that these scavengers also contributed to the photoinduced disinfection process. The addition of the inhibitor, isopropanol, on the other hand, had no inhibitory effect on the bacterial inactivation process, demonstrating that ·OH had no function in the sterilization process. SPR response of AuNPs contributed to improved photon harvesting capabilities and the development of numerous electron-hole couples. Previous research

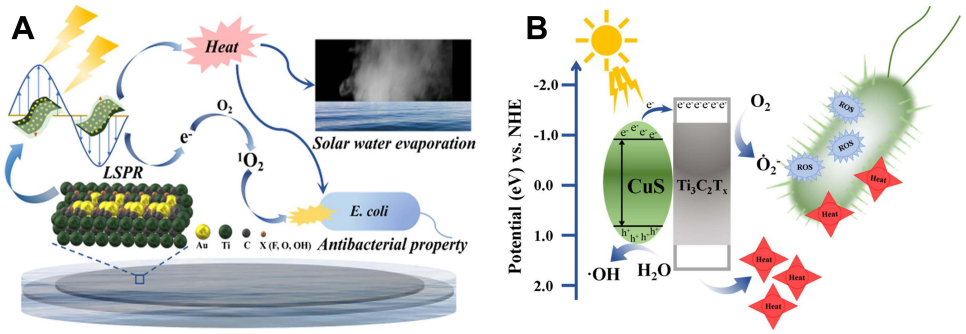

Figure 5 (**A**) Photodynamic antibacterial pathway of the gold/Ti_3C_2 photoactive membrane. Reprinted with permission from Qu W, Zhao H, Zhang Q, et al. Multifunctional Au/ti3c2 photothermal membrane with antibacterial ability for stable and efficient solar water purification under the full spectrum. *ACS Sustain Chem Eng*. 2021;(9):11372–11387, Copyright (2021). American Chemical Society.[83] (**B**) Antibacterial pathway of titanium carbide ($Ti_3C_2T_x$)@copper sulfide under solar light irradiation. Reprinted from *J Colloid Interface Sci*. Volume: 604. Li Q, Wang W, Feng H, et al. Nir-triggered photocatalytic and photothermal performance for sterilization based on copper sulfide nanoparticles anchored on ti3c2tx mxene. 810–822, Copyright (2021), with permission from Elsevier.[84]

revealed that the photodynamic behavior of Ti_3C_2/PF $^1O_2$ generation was similar to that of black phosphorus and graphene quantum dots. Under light illumination, Ti_3C_2/PF generates photoinduced electrons and subsequently transfers energy to the ground-state oxygen, $^3O_2$, to generate $^1O_2$ species. Similarly, because of the SPR effect, AuNPs can generate ROS when exposed to light. The Au/Ti_3C_2 photoactive membrane also showed good photoactive antibacterial capabilities, inactivating 6.7 log10 colony-forming units (CFU) mL^{-1} *E. coli* K-12 in 20 min and 7.1 log10 CFU mL^{-1} *Sphingopyxis* sp. BM1-1 in 10 min.[78–83]

To achieve an effective antibacterial effect, a new photocatalytic antibacterial material was developed, and its mechanism of action is shown in Figure 5B. Titanium carbide ($Ti_3C_2T_x$)@copper sulfide (CuS) composites were created using a straightforward hydrothermal technique in which CuS NPs were attached to the surface of Ti_3C_2Tx to significantly improve its photocatalytic and antibacterial properties. $Ti_3C_2T_x$@CuS had 99.6% bactericidal activity against *E. coli* and 99.1% bactericidal activity against *S. aureus*. CuS is a p-type semiconductor that is stimulated by a light source to cause hybridization. Excited electrons exit, forming electron-hole pairs. When electrons and holes are separated, they can interact with O_2 and H_2O to form ROS such as superoxide and hydroxyl radicals. The transfer of excited electrons to the conductive $Ti_3C_2T_x$ after CuS is compounded with it enhances the separation of electrons and holes and boosts the ROS-generating ability. The $Ti_3C_2T_x$@CuS heterojunction offers a wide range of potential applications in the decontamination and antimicrobial domains.[84–86]

Photothermal Antibacterial Therapy

Mechanistic Overview of Photothermal Therapy

PTT is one of several ways developed as an innovative strategy to tackle infectious diseases in response to resistance to antibiotics.[87] When photoresponsive nanomaterials are activated with a suitable NIR laser, the plasmon resonance band causes the conversion of electromagnetic energy to heat. The resultant heat can reach levels high enough to kill bacterial cells. The photothermal effect causes membrane damage, which leads to protein inactivation and/or leakage, ultimately leading to bacterial mortality (Figure 6).[88–90] PTT is effective against both gram-positive and gram-negative bacteria, independent of bacterial resistance. It is rapid, non-intrusive, and accurate, and can be regulated by the incident light and duration of irradiation. PTT, moreover, can be used with other therapies like PDT, chemotherapy, radiation, and so on to improve treatment outcomes. As a result, numerous photothermal NPs or nanostructures are being produced to treat bacterial diseases. Photothermal therapy agents are photothermal NPs that are classified as metallic materials, metal sulfides, oxides, carbon-based nanostructured materials, small molecule-based nanomaterials, and polymeric NPs. When compared to inorganic or organic photothermal therapy agents, a group of transition metals and their oxide and sulfide forms can absorb more laser energy.[91–96] Furthermore, PTT is considered as one of the most promising methods when combined with transition metals for disinfection and effective antimicrobial activity.

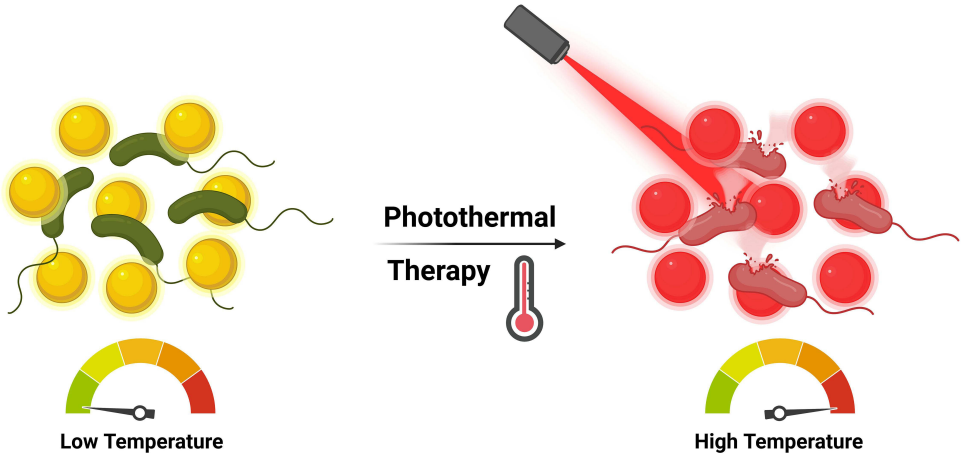

Figure 6 Schematic illustration of the photothermal antibacterial pathway of nanomaterials.

Photothermal Mechanisms of TMNs

In our recent study, under NIR light irradiation, the photothermal mode of action of CuS NPs was elucidated.[54] According to our findings, reducing the size of covellites increased the photothermal efficiency and enhanced the photothermal antibacterial activity (Figure 7A). As previously stated, CuS NSs and CuS NPs were photodegraded for 5 min with NIR laser irradiation, resulting in hazardous copper ions. The heat and radicals produced by copper ions and carbon residues had a negative influence on *E. coli* cell envelopes. The synthesis of copper ions was corroborated by UV spectra of CuS NSs and CuS NPs following NIR laser irradiation, which revealed an upsurge in absorption intensities in the NIR region resulting in the release of copper ions and the development of heat. CuS NPs outperformed their counterparts because of their higher thermal efficiency due to their smaller size, which caused significant damage to *E. coli* when exposed to NIR laser light. As a result, copper ions generated by CuS NSs and CuS NPs using an NIR laser reacted with ambient moisture and oxygen to form ·OH and $\cdot O_2^-$ radicals. Under NIR laser irradiation, the created radicals coupled with higher thermal efficiency and variations in size (reductions) of CuS NSs and CuS NPs to reasonably boost the antibacterial efficiency. Furthermore, the thermal efficiency and diameters of CuS NSs and CuS NPs were shown to be connected to *E. coli* growth and thermal curves.[97–99]

Furthermore, we quantified adsorption energies of 1T- and 2H-MoS_2 systems, and it was discovered that the adsorption energy of the substrates was in the order of 1T-MoS_2<2H-MoS_2, implying that moisture was easily desorbed from the 1T-MoS_2 system for photothermal heating, demonstrating a further antimicrobial effect.[54] The electronic effect was demonstrated by analyzing water adsorption. Chemical characteristics of TM surfaces are significantly influenced by

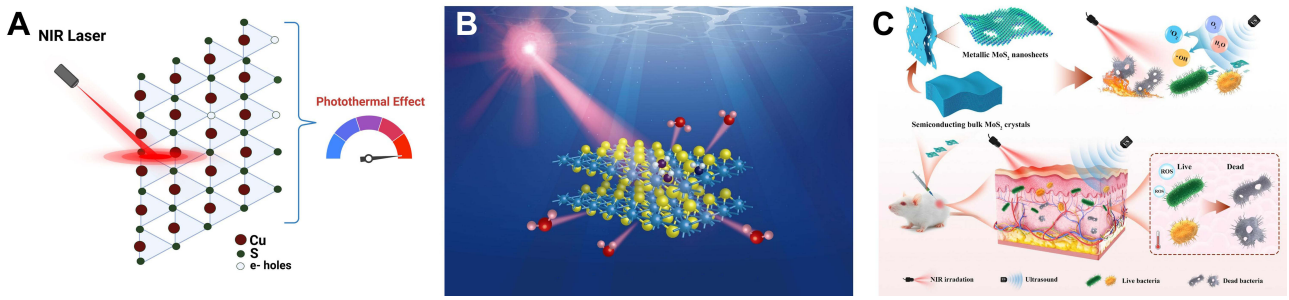

Figure 7 (**A**) Photothermal antibacterial pathway of copper sulfide nanosheets. Reprinted from *J Colloid Interface Sci*. Volume: 607. Mutalik C, Okoro G, Krisnawati DI, et al. Copper sulfide with morphology-dependent photodynamic and photothermal antibacterial activities. 1825–1835, Copyright (2022), with permission from Elsevier.[54] (**B**) Antibacterial mechanism of 1T- and 2H-MoS_2 nanosheets (NSs) by photothermal therapy. Reprinted with permission from Mutalik C, Okoro G, Chou HL, et al. Phase-dependent 1T/2H-MoS2 nanosheets for effective photothermal killing of bacteria. *ACS Sustain Chem Eng*. 2022;(10):8949–8957. Creative common.[100] (**C**) MoS_2 NSs (metallic 1T/1T' or semiconducting 2H), and their crystal-phase effects on photothermally enhanced sonodynamic antibacterial treatments as investigated by in vitro and in vivo methods. Reproduced with permission from Chen H, He X, Zhou Z, et al. Metallic phase enabling MoS2 nanosheets as an efficient sonosensitizer for photothermal-enhanced sonodynamic antibacterial therapy. *J Nanobiotechnol*. 2022;(20):136. Creative Common.[110]

the various absorption coefficients linked to adsorbates at surface imperfections. Catalytic activity and selectivity are altered, as are material properties, a significant consequence in chemical nanotechnology. According to Density Functional Theory simulation estimates, 1T-MoS_2 NSs have higher antibacterial potential than 2H-MoS_2 NSs. The crystal phase-dependent abilities of 1T- and 2H-MoS_2 NSs were investigated using *E. coli* as a bacterial model. Moreover, considering the metallic characteristics of 1T-MoS_2 NSs, it is likely that when irradiated, they produce far more detectable antibacterial effects than semiconducting 2H-MoS_2 NSs. The metallic character of 1T-MoS_2 NSs indicates stronger conductivity of the material, which may result in a lower electron transport barrier across bacteria in the surroundings and their intracellular components, resulting in the reported bacterial toxicity of NSs. However, the intrinsic great NIR absorbance potential of 1T-MoS_2 NSs results in significant bacterial destruction. Figure 7B shows the photothermal capability of MoS_2 NSs by demonstrating the mechanism of action of adsorption and desorption of metal ions and atmospheric moisture.[100–109]

Moreover, several phases of MoS_2 nanosheets (metallic 1T/1T' or semiconducting 2H) were prepared, and their crystal-phase effects on photothermal-enhanced sonodynamic antibacterial treatments were investigated by in vitro and in vivo methods.[110] Figure 7C shows a mechanistic overview carried out in that study. Additionally, the ultrasound (US)-induced ROS generation performance of the M-MoS_2 nanosheets was further improved by a photothermal effect under 1064-nm laser ablation due to its metallic phase-enabled strong absorption in the NIR-II regime. Notably, compared to semiconducting 2H-phase MoS_2 nanosheets, the defective 2D MoS_2 nanosheets with high percentages of the metallic 1T/1T' phase (referred to as M-MoS_2) exhibited massively greater activity towards the US-induced formation of ROS. The M-MoS_2 nanosheets can thus be utilized as an effective sonosensitizer for photothermally enhanced sonodynamic bacterial eradication when US treatment is combined with NIR-II laser irradiation following modification with polyvinylpyrrolidone (PVP). The plate count method was used to investigate the antimicrobial effect of the PVP-modified M-MoS_2 nanosheets against *Pseudomonas aeruginosa* and *S. aureus*. In contrast to the control and M-MoS_2 groups, the M-MoS_2 + laser + US group showed significantly better bactericidal effects. Their research illustrates the potential of metallic MoS_2 nanosheets as a photothermally enhanced sonosensitizer for antibacterial therapy. The photothermally increased sonodynamic performance of nanomaterials is also strongly influenced by their crystal phase, making metallic MoS_2 a viable photosensitizer for antibacterial uses.[111–116]

Recently, for attaining rapid NIR laser-induced sanitation, a novel antimicrobial nanoplatform centered on quaternized chitosan (QCS)/silver (Ag)/cobalt phosphide (CoP) nanocomposites was developed against *E. coli* and *S. aureus*. In core-shell combinations, Ag NPs with a size of 25 nm were consistently placed on CoP nanoneedles, which were then capped with a layer of QCS (about 10%). Under laser irradiation, high thermally conductive electrons resulting from an SPR phenomenon of Ag transited into the junction between Ag and CoP, amplifying the photothermal effect of CoP, according to parametric studies. Furthermore, since the Schottky heterostructure enhances ROS generation, photoexcited electrons from CoP were transferred onto Ag NPs. Ag loading simultaneously boosted photocatalytic and photothermal actions of CoP, resulting in a combinatorial antimicrobial effect. In a nutshell, Figure 8A depicts the photocatalytic mechanism. This metal-semiconductor heterostructure (Ag/CoP nanostructure) may be considered an appropriate Schottky junction since the CB position of CoP vs the NHE is 0.43 eV, which is higher than the Fermi level of Ag (0.24 eV). The VB electrons of CoP are stimulated to the CB and create electron-hole pairs when Ag/CoP is subjected to 808-nm light. As a result of the Schottky junction and high conduction ability of the Ag NPs, photoinduced electrons from CoP are rapidly transported to the surface of the Ag NPs, resulting in improved electron-hole pair removal efficiency and ROS production.[117–122]

The development of a multi-functional platform capable of promptly and sensitively detecting bacteria and effectively inhibiting or killing germs is critical and essential. A novel flexible MXene-Au nanocomposite for rapidly detecting germs and photothermally sterilizing them was successfully manufactured using a self-assembly approach. Gram-negative *E. coli* and gram-positive *Bacillus subtilis* were employed as models for label-free, quick, and sensitive bacterial detection using the surface-enhanced Raman spectroscopic (SERS) approach. A colony counting method was used to demonstrate the material's antibacterial effectiveness; *E. coli* and *B. subtilis* survival rates were as low as 8.05% and 0.06%, respectively. Within 6 min, the 808-nm light-irradiated Ti_3C_2Tx-Au NPs had a considerable antibacterial impact, with 100% and 99.25% germicidal rates for *B. subtilis* and *E. coli*, respectively. The efficiency of photothermal

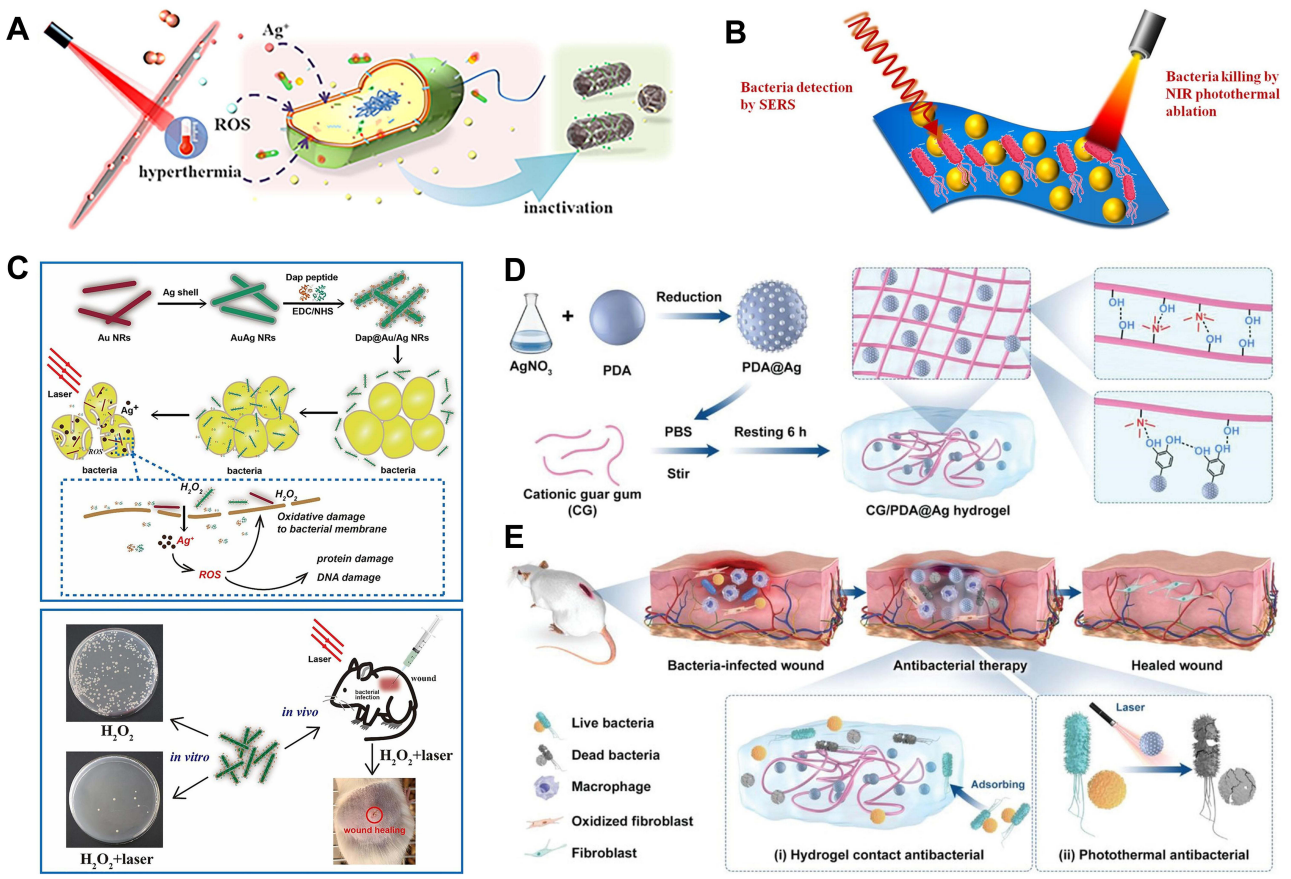

Figure 8 (**A**) Schematic representation of photothermal antibacterial pathway of quaternized chitosan (QCS)/silver (Ag)/cobalt phosphide (CoP) nanocomposites. Reprinted from *J. Colloid Interface Sci.* Volume: 616. Han H, Xu X, Kan H, et al. Synergistic photodynamic/photothermal bacterial inactivation over heterogeneous quaternized chitosan/silver/cobalt phosphide nanocomposites. 304–315, Copyright (2022), with permission from Elsevier.[117] (**B**) The photothermal antibacterial pathway and surface-enhanced Raman scattering for bacterium detection by MXene-gold (Au) nanocomposites. Reprinted from *Chem Eng J*. Volume: 426. Yu Z, Jiang L, Liu R, et al. Versatile self-assembled mxene-Au nanocomposites for SERS detection of bacteria, antibacterial and photothermal sterilization. 131914, Copyright (2021), with permission from Elsevier.[123] (**C**) Synthesis, in vitro photothermal antibacterial pathway, and in vivo wound healing and disinfection of Dap@gold/silver nanorods (Au/Ag NRs). Reprinted from *Chem Eng J*. Volume: 432. Dong X, Ye J, Chen Y, Tanziela T, Jiang H, Wang X. Intelligent peptide-nanorods against drug-resistant bacterial infection and promote wound healing by mild-temperature photothermal therapy. 134061, Copyright (2022), with permission from Elsevier.[135] (**D**) Diagram showing the creation of CG/PDA@Ag hydrogel and its use as a photothermal antibacterial platform for treating wounds. (**E**) Using a simple one-pot mixing infusion method, a strong hydrogel dressing was easily produced that can speed up wound healing by a combination of photothermal and synergistic antibacterial therapies. (**D** and **E**) Reprinted with permission from Qi X, Huang Y, You S, et al. Engineering robust Ag-decorated polydopamine nano-photothermal platforms to combat bacterial infection and prompt wound healing. *Advanced Science*. 2022;(9):2106015. © 2022 The Authors. Advanced Science published by Wiley-VCH GmbH.[143]

conversion increased to 43.40%. Therefore, this multi-functional nanocomposite material offers a highly promising countermeasure for the clinical treatment of diseases brought on by MDR bacteria. It not only has sensitive bacterial detection capabilities but also has antimicrobial and photothermal sterilization effects (Figure 8B).[123–134]

Recently, a novel antimicrobial nanosystem based on gold (Au) nanorods (NRs) called Dap@Au/silver (Ag) NRs was studied for its photothermal antibacterial capabilities using an experimental strain of MRSA. By releasing significant numbers of silver ions and antimicrobial peptides (Dap) when exposed to H_2O_2, Dap@Au/Ag NRs greatly compromised the integrity of MRSA membranes, causing content leakage and bacterial demise. Additionally, in vivo and in vitro tests revealed that the antibacterial mechanistic actions of Dap@Au/Ag NRs were greatly enhanced by utilizing AuNRs with a good photothermal effect after being exposed to a specific amount of laser irradiation (808 nm, 0.8 W/cm^2, for 40~60s) (Figure 8C). In contrast to conventional PTT, it was discovered that when laser irradiation was administered in the early stages of infection and under mild temperature control (below 47°C), this not only notably demonstrated bacteriostasis of MRSA, prevented large areas of wound ulceration, and promoted wound healing, but it also had no evident thermal deformation at the incision site or surrounding skin. These findings demonstrated the significant bactericidal properties of the novel Dap@Au/Ag NR antibacterial nanosystem, which can be used as a potential promising antimicrobial agent.

This finding offers a fresh approach for facilitating and enhancing the antimicrobial efficiency to prevent drug-resistant bacterial infections.[116,135–142]

The recent synthesis of polydopamine@silver (PDA@Ag) NPs involved culturing Ag on the surface of PDA NPs, which was followed by their encapsulation in a network of cationic guar gum (CG) hydrogels. When compared to pure PDA, the optimized CG/PDA@Ag platform's photothermal conversion efficiency (38.2%) was more than twice as high (16.6%). More importantly, the designed CG/PDA@Ag hydrogel's many active groups effectively interacted with bacteria to trap and kill them, enhancing the antibacterial effect. As expected, it was shown that the developed CG/PDA@Ag system, which combined the benefits of PDA@Ag NPs (with high photothermal conversion efficiency (PCE)) and hydrogel (preventing PDA@Ag NP aggregation and having an innate antibacterial ability), had better antibacterial efficacy both in vitro and in vivo. According to antibacterial tests, this composite CG/PDA@Ag hydrogel was 99.9% effective against *E. coli* and 99.1% effective against *S. aureus*. An environmentally friendly, simple, broad-spectrum, and highly effective antibacterial platform was mechanically developed as a result of the high PCE and inherent bacterial capture/killing ability of the hydrogel matrix. This platform not only ensured high-efficiency bacteria-killing ability toward *E. coli* (99.9%) and *S. aureus* (99.8%) in vitro but also realized outstanding potent antimicrobial activity in vivo. The preparation and photothermal mechanism of action are shown in Figure 8D and E.[143–150]

Metal Ion Release

Mechanistic Overview

Numerous chemical and physical characteristics of metal ions characterize their mechanisms of cell toxicity. Mn^{+} can interact with a variety of bacterial cell targets, such as DNA, membranes, and enzymes. Depending on variables including temperature, pH, ionic strength, binding partners, and the reduction potential of the immediate environment, they can exist as a variety of distinct chemical species. For instance, in contrast to the periplasm of gram-negative bacteria, the cytoplasm is a potent reducing environment. The oxidation state of metals and, consequently, metal speciation are greatly impacted by this. Metals are also often not widely accessible inside cells. Instead, a sophisticated network of transporters, metalloregulatory sensors, and metallochaperones control the availability and speciation of metals and enable the directed transport to, for example, metalloproteins. Metal speciation generally has a significant impact on a metal's bioavailability and responsiveness, making it a key physicochemical characteristic of metal toxicity.[151–154] Metallic (M)-NPs are inorganic particles with diameters between 1 and 100 nm with a variety of forms (eg, spheres, triangles, sheets, plates, tubes, cubes, and rods). Importantly, recent studies revealed that a variety of variables, including the M-NPs' size, charge, zeta potential, surface morphology, and structure, may affect their antibacterial properties. M-NPs' tiny size is a huge benefit for achieving powerful antibacterial action in the struggle against microorganisms. Smaller M-NPs, for instance, often exhibit better antibacterial activity as a result of their relatively larger surface-to-volume ratios, which enhance their capacity to create ROS, which can then destroy bacterial components. Previous studies have demonstrated that smaller-sized particles can effectively interact with bacterial membranes because of their large surface area to result in enhancing their antibacterial activities.[155–158] The shape of M-NPs that have the same surface-to-volume ratios is equally essential, with nanotubes and rods being more effective since their planes are exposed, allowing the metals to oxidize. By electrostatic contacts, van der Waals forces, receptor-ligand interactions, and hydrophobic interactions, NPs first cling to bacterial membranes. Following contact, the M-NPs can cross the bacterial membrane, impede metabolic processes, and alter the structure and function of the membranes. M-NPs have the ability to alter gene expression levels, create oxidative stress, inhibit enzymes, and deactivate proteins once they have entered cells. A crucial stage in the development of metal toxicity is thought to be the accumulation of a metal inside the bacterium (Figure 9).[159–166]

Metal Ion Release Mechanisms of TMNs

A variety of polyamide (PA)-based membranes designed with unique metal ions (Cu^{2+} and Fe^{3+}) for forward osmosis (FO) separation were manufactured via one-step metal-ligand ligation. Membranes with improved performance, and higher water permeability and selectivity were synthesized using a novel approach. Compared to nascent PA membranes

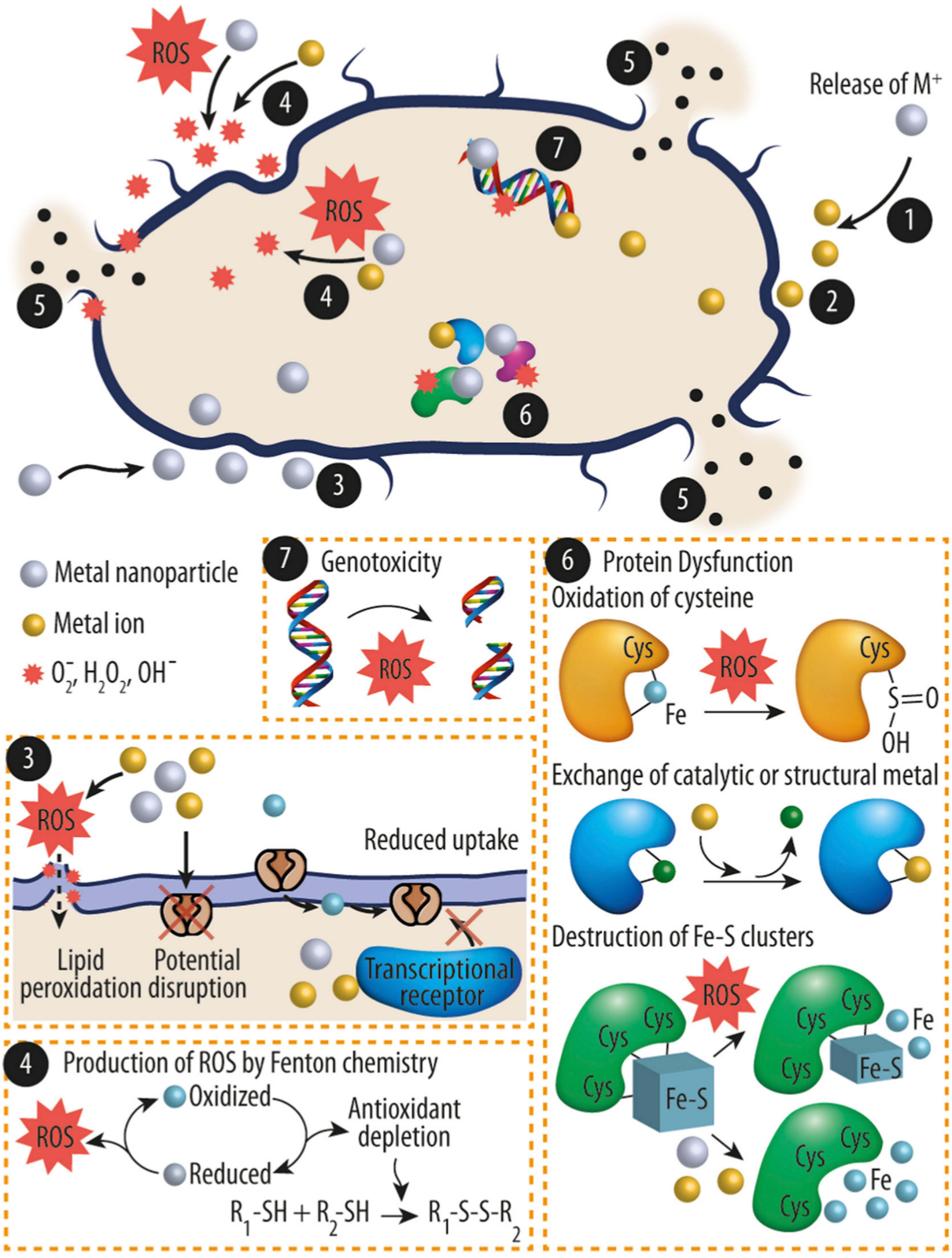

Figure 9 Schematic illustrations of the antibacterial mechanisms for metal ions and nanoparticles. The primary modes of action are: (1) metal ion release from metal nanoparticles and (2) direct interactions of the metal ions and/or (3) metal nanoparticles with the cell wall via electrostatic interactions, leading to impaired membrane function and nutrient assimilation; (4) formation of extracellular and intracellular reactive oxygen species (ROS) and oxidative stress damage to lipids, proteins, and DNA; (5) high levels of metal-binding to cell walls and reactive species which can damage cell components; and (6, 7) absorbed metals, nanoparticles, or metal ions might interfere with functional proteins and DNA of bacteria causing severe damage and lead to death. Reprinted from *Bioactive Materials*. Volume: 6. Godoy-Gallardo M, Eckhard U, Delgado LM, et al. Antibacterial approaches in tissue engineering using metal ions and nanoparticles: From mechanisms to applications. 4470–4490, Copyright (2021). Open Access.[165]

in a 0.5 M saline solution, the Fe^{3+} membrane enhanced water flows by 93% (in the FO mode) and 112% (in the pressure retarded osmosis mode). Cu^{2+} and Fe^{3+} on the membrane surface boost bactericidal activity against *E. coli* by damaging the bacterial phospholipid layer.[167] The antimicrobial activity and mechanisms of the membranes created here have been thoroughly studied. Both Cu^{2+} and Fe^{3+} have bactericidal efficiency against *E. coli*; however, Cu^{2+} has better antibacterial potential than Fe^{3+}, according to the findings. Moreover, Cu-M and Fe-M metal-ion functionalized membranes were produced by a one-step synthesis under moderate circumstances. The hydrated layer based on metal ions increases the physicochemical and structural aspects of the membranes produced. Compared to PA-M, Cu-M and Fe-M have significantly better extraction efficiencies and antibacterial activities (Figure 10). Furthermore, compared to PA-M, Fe-M has a better desalination efficiency by more than 68%. Cu-M and Fe-M have substantially better antibacterial characteristics than PA-M due to their combined actions. *Escherichia coli* on the PA-M surface has a characteristic small rod shape with an intact cytomembrane. Bacteria on Cu-M and Fe-M surfaces, on the other hand, shrink to a considerably smaller oval shape with a withered surface. This implies that the *E. coli* cytomembrane has been disrupted, allowing nutrients to escape and causing the bacterium to grow abnormally, resulting in a distorted shape. Suppression of the growth of bacteria by Cu^{2+} or Fe^{3+} causes these alterations in the membrane surfaces of *E. coli*. Electrostatic attraction drives Cu^{2+} or Fe^{3+} to *E. coli* cell walls, where it is absorbed and accumulates. Cu^{2+} then reacts with both phospholipids on the cytomembrane and proteins and DNA within the bacterium, modifying the physical and chemical properties of the cells and producing an antibacterial action. Fe^{3+} on the *E. coli* cytomembrane surface, unlike Cu^{2+}, is more likely to form radicals which can induce oxidative stress, that then damages the bacterial shells through numerous intermolecular interactions, inhibiting bacterial growth and differentiation and eventually leading to bacterial mortality.[165,167–174]

In Figure 11, the action of Ag NPs synthesized using a plant source and release of silver ions which caused substantial bacterial cell damage and biofilm growth inhibition is illustrated. The first stage of an *Acinetobacter baumannii* infection is colonization, particularly when the bacterium is adhering to epithelial cells. There are several other types of cell-surface adhesions that can occur, such as pill-like structures, fimbrial-like structures, and the attachment of the bacterial outer membrane protein A to fibronectin and unidentified receptors on the surface of the host cell. Organisms can tightly

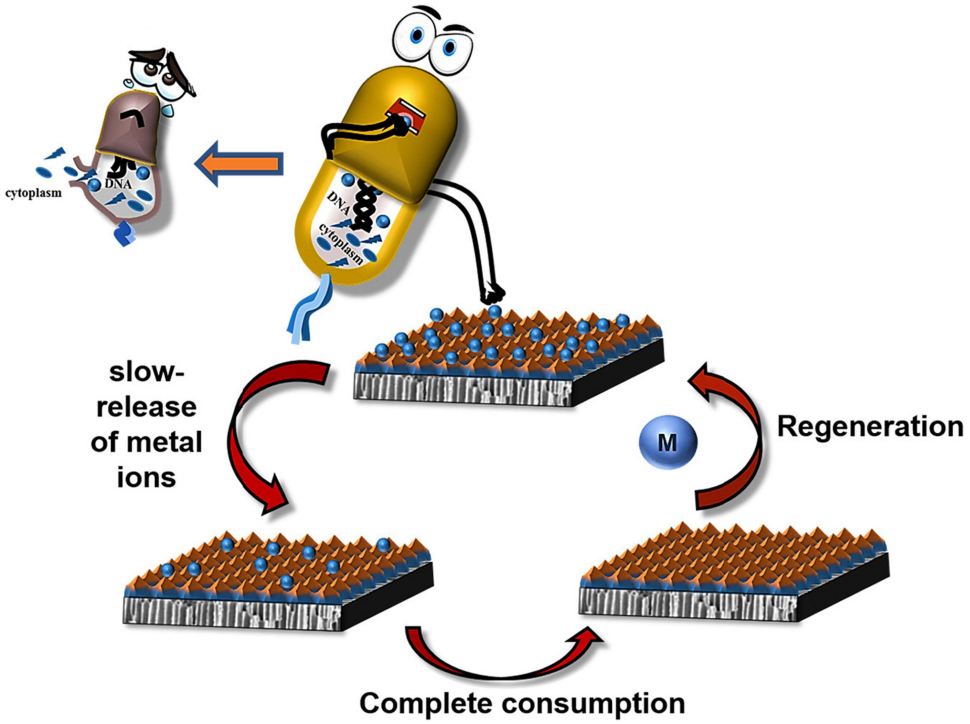

Figure 10 The antibacterial mechanism of metal ion-functionalized membranes is depicted schematically. Reprinted from *Desalination*. Volume: 530. Tang X, Hu W, Ke X, Zheng Y, Ge Q. Antibacterial and desalting behavior of forward osmosis membranes engineered with metal ions. 115655, Copyright (2022), with permission from Elsevier.[167]

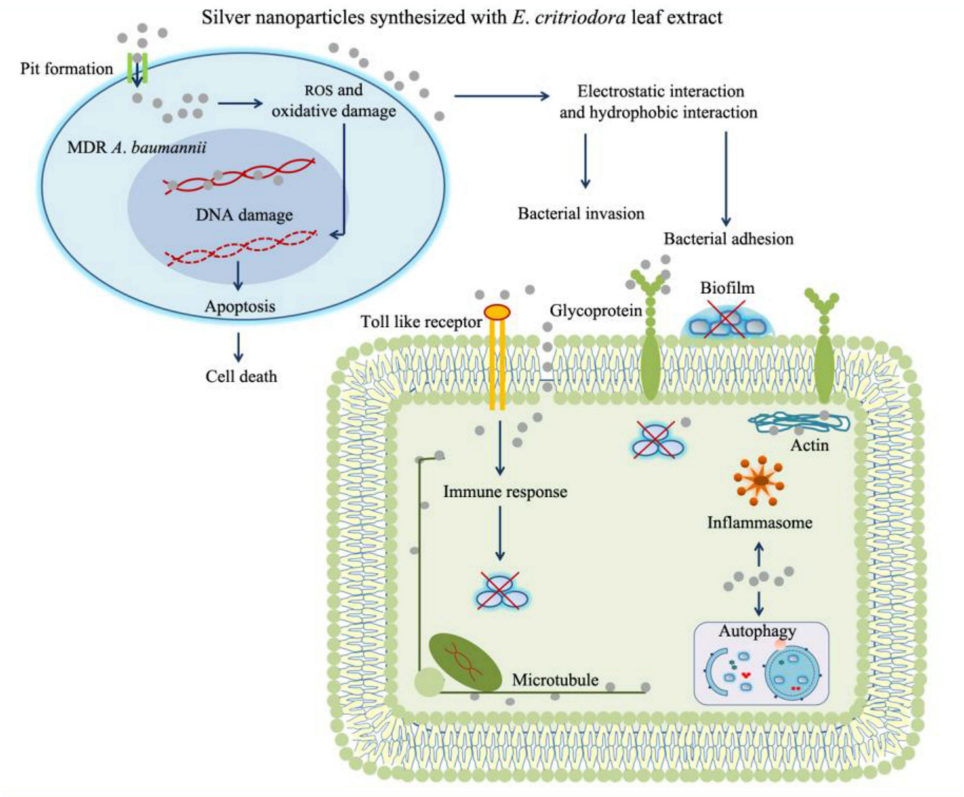

Figure 11 Silver nanoparticles made using an *Eucalyptus citriodora* ethanol leaf extract increase the antimicrobial property against clinically multidrug-resistant *Acinetobacter baumannii* isolated from pneumonia patients, as shown in the schematic. Reprinted from *Microbial Pathogenesis*. Volume: 126. Wintachai P, Paosen S, Yupanqui CT, Voravuthikunchai SP. Silver nanoparticles synthesized with eucalyptus critriodora ethanol leaf extract stimulate antibacterial activity against clinically multidrug-resistant acinetobacter baumannii isolated from pneumonia patients. 2019, 126, 245–257, Copyright (2019), with permission from Elsevier.[175]

adhere to plasma membranes thanks to these interactions, which eventually allow for colonization and invasion of host cells. According to reports, the degree of bacterial hydrophobicity or electrostatic contact has a significant role in bacterial infection for cells related to bacteria.[175] It was observed that the proportion of MDR clinical isolates of *A. baumannii*-linked A549 cells was inhibited by Ag NPs produced from the *Eucalyptus citriodora* leaf extract. The bacterial cell surface may be affected by Ag NPs made from the *E. citriodora* leaf extract, including a conduction sticky factor like the level of bacterial hydrophobicity, which is followed by a decrease in the number of microbial cells. Furthermore, the decrease in *A. baumannii*-associated cells is probably partly the result of mechanisms that reduce bacterial pathogenicity, like the creation of biofilms. It is interesting to note that polypeptide glycosylation was found to increase the production of biofilms in *A. baumannii*. It was also suggested that protein glycosylation may affect how cells and NPs interact, resulting in the uptake of NPs by cells. Together, these interactions may prevent microbial cells from proliferating and bacterial invasion. In this study, *A. baumannii* infestation levels were reduced without cell cytotoxicity by Ag NPs made using an *E. citriodora* leaf extract. Although it was suggested that Ag NPs can activate adaptive and innate immune systems by binding to toll-like receptors, bacteria need the host cell's cytoskeleton as their destination for intracellular access and penetration. It was demonstrated that Ag NPs bind to the cytoskeletal proteins, tubulin and actin, and that this binding might result in bacterial inhibition.[175–185]

In a recent study similar to previous ones,[175] Figure 12A shows the silver ion release and destruction of the bacterial cell wall in a different host (MRSA).[186] Owing to its special ability to interact with bacterial cell surfaces without having to penetrate them, nanosilver promises to continue to play a more significant role in bactericides than antibiotics. The total bioactivity of a protein or enzyme may be impacted by conformational changes brought on by nanosilver. Dihydrolipoamide dehydrogenases (SAV1518 and E3) transport galactose and have the highest confidence score (0.788), suggesting that nanosilver strongly interacts with transport proteins compared to other proteins. Additionally,

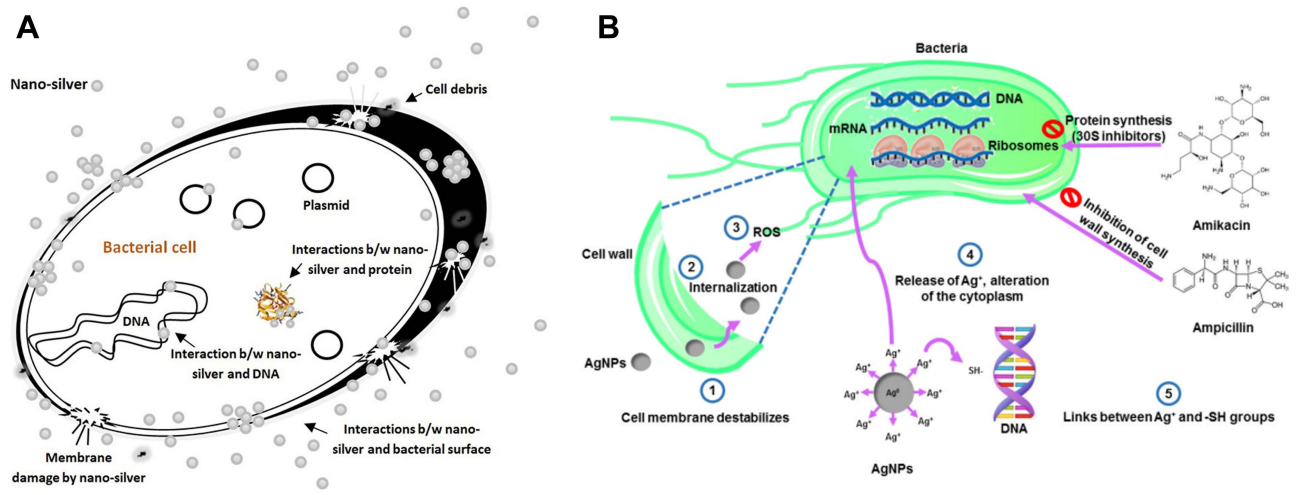

Figure 12 (**A**) Schematic illustration of silver ion release and destruction of the bacterial cell wall in methicillin-resistant *Staphylococcus aureus* (MRSA). Reprinted from *European Journal of Pharmaceutical Sciences*. Volume: 127. Anuj SA, Gajera HP, Hirpara DG, Golakiya BA. Interruption in membrane permeability of drug-resistant staphylococcus aureus with cationic particles of nano-silver. 208–216, Copyright (2019), with permission from Elsevier.[186] (**B**) Schematic and step-by-step illustration of silver ion internalization and damage to DNA and functional proteins in bacteria. Reprinted with permission from Lopez-Carrizales M, Velasco KI, Castillo C, et al. In vitro synergism of silver nanoparticles with antibiotics as an alternative treatment in multiresistant uropathogens. *Antibiotics*. 2018;(7):50, Open Access.[193]

nanosilver interacts with transport proteins like the ATP-binding cassette transporter, SAV2623, and the permease transporter, SAV1549, which suggests that nanosilver may prevent bacteria from transporting certain materials. Any change in surface charges may modify the permeability of the cell surface, which might further result in cell death. In an investigation, it was discovered that normal and autoclaved strains of *S. aureus* MTCC 3160 had average zeta potentials of 50.2 and 3.2 mV, respectively. The findings showed that nanosilver at a concentration of 100 g/mL could change the zeta potential. Bacterial cells contacting nanosilver produced structural effects that destroyed the bacterial membranes and caused the cells to leak some internal components. Nanosilver was previously found to cause this kind of toxicity that is mediated by membrane depolarization. As was demonstrated by interactions between positively charged nanosilver and bacterial proteins, alteration of the zeta potential of cell surfaces may be related to both positively charged nanosilver and bacterial surface proteins. Those findings revealed that nanosilver may harm bacterial DNA, causing loss of multiplication and ultimately leading to the death of the *S. aureus* MTCC 3160 bacterium.[186–192]

Figure 12B shows the antibacterial mechanism of Ag NPs releasing silver ions which caused severe damage to and death of microbial pathogens. The need for new therapeutic techniques against MDR pathogens, such as the combination of selected antimicrobials, can be viewed as a viable option. By maximum inhibitory concentration assays and checkerboard testing, the in vitro activities of two groups of conventional antimicrobial agents alone and combined with AgNPs were investigated against a set of ten MDR clinical isolates and two reference strains, as well as their cytotoxicity toward human fibroblasts by an MTT assay at the same concentration of the antimicrobial agents alone and in combination. By identifying the lactate dehydrogenase activity associated with respiration in *E. coli* and *S. aureus*, the nanosilver inhibited the respiration process. Additionally, they discovered that hydrogen atoms from the thiol group of cysteine was replaced with positively charged nanosilver, which prevented the dehydrogenase's action thus killing the bacteria. It is thought that nanosilver may disrupt bacterial membranes and interfere with respiratory dehydrogenases, killing bacteria by inhibiting their respiratory system.[193–197] At the end of this part, we have collected recent achievements by the uses of TMNs with photodynamic, photothermal, and metal ion release antibacterial applications as shown in Table 1.

Challenges, Opportunities, and Conclusions

The current review article brings together recent achievements in photodynamic, photothermal, and ion release antibacterial therapeutics using transition metal nanomaterials and their composites. These nanostructures could soon bring promising antimicrobial prospects to food storage, wastewater treatment, and medication, according to findings of these investigations. Transition metals, transition metal-polymer nanocomposites, transition bimetallic nanoparticles, and other promising

Table 1 Summary of Photodynamic, Photothermal, and Metal Ion Release Antibacterial Pathways by TMNs

TMNs	Mechanism	Light Source	Bacterium	Reference
CuS nanosheets	PDAT	Simulated solar light	*E. coli*	[88]
1T-MoS_2 nanoflowers	PDAT	Simulated solar light	*E. coli*	[46]
TiO_2/FeS_2 nanocomposites	PDAT	Simulated solar light	*E. coli*	[51]
TiOx-Au nanocomposites (50:1)	PDAT	Simulated solar light	*E. coli*	[56]
			MRSA	
MnO_2/ZIF-8	PDAT	Simulated solar light	*E. coli*	[62]
			MRSA	
Au/Ti_3C_2 photoactive membrane	PDAT	Simulated solar light	*E. coli*	[71]
			Sphingopyxis sp.	
Ti_3C_2Tx@CuS	PDAT	Simulated solar light/red light	*E. coli*	[72]
			S. aureus	
CuS nanoparticles	PTAT	NIR	*E. coli*	[88]
QCS/Ag/CoP nanocomposites	PTAT/PDAT	NIR	*E. coli*	[106]
			S. aureus	
MXene-Au nanocomposites	PTAT	NIR	*E. coli*	[112]
			B. subtilis	
1T/2H-MoS_2 nanosheets	PTAT	NIR	*E. coli*	[89]
Dap@Au/Ag NRs	PTAT	NIR	MRSA	[113]
MoS_2 nanosheets	PTAT/ SDT	NIR	*P. aeruginosa*	[90]
			S. aureus	
CG/PDA@Ag hydrogel	PTAT	NIR	*E. coli*	[114]
			S. aureus	
Cu- and Fe-membrane	MIR	N/A	*E. coli*	[153]
Ag nanoparticles	MIR	N/A	*A. baumannii*	[161]
Nanosilver	MIR	N/A	MRSA	[172]
Ag nanoparticles	MIR	N/A	*E. coli*	[179]
			S. aureus	

Abbreviations: TMNs, transition metal-based nanocomposites; PDAT, photodynamic antibacterial therapy; PTAT, photothermal antibacterial therapy; SDT, sonodynamic therapy; MIR, metal ion release; NIR, near infrared; Ag, silver; Au, gold; Cu, copper; Fe, iron; Dap, peptide; PDA, polydopamine; CG, cationic guar gum; NPs, nanoparticles; Ti_3C_2Tx/MXene, titanium carbide; CuS, copper sulfide; MoS_2, molybdenum disulfide; CoP, cobalt phosphide; N/A, not applicable; *E. coli, Escherichia coli*; MRSA, methicillin-resistant *Staphylococcus aureus; S. aureus, Staphylococcus aureus; B. subtilis, Bacillus subtilis; P. aeruginosa, pseudomonas aeruginosa; A. baumannii, Acinetobacter baumannii.*

antibacterial agents can be used for such applications. The antibacterial processes, ROS-generating abilities, and microbial inhibition of photodynamically active transition metal nanomaterials recently explored were demonstrated using artificial sunlight irradiation or equivalent lighting fixtures. The photothermal impacts of transition nanomaterials were demonstrated in vitro and in vivo by detailing the active processes and thermal efficiencies. In addition to their improved thermal efficiencies under NIR light exposure, the nanostructures influence bacterial bioactivities through their photothermal effects. Metal ion release is analogous to photodynamic activity in the dark and is entirely dependent on the solubility and dissolution of metal nanoparticles to produce ROS and may have antimicrobial and antibiofilm effects. One of the most important unresolved problems is the therapeutic acceptance of these metallic nanostructures and their ability to limit bacterial growth (they are required to exhibit a 4-log reduction or about 99.99% efficiency). Another critical topic that remains unresolved is the toxicology and biocompatibility of these metallic nanostructures. To improve treatment outcomes, PTT can be combined with several other treatments such as metal ion release, PDT, chemotherapy, sonodynamic therapy, radiation, and so on. Bacterial infestations are projected to be the most common diseases that need to be contained globally, and analyzing the safety and efficacy of accessible nanomaterials will be critical prior to their use in human organisms and also assessing their potential substantial effects on ecosystems.

Acknowledgments

We thank the financial support from the National Science and Technology Council, Taiwan (grant no.: MOST 111-2113-M-038-003), Taipei Medical University, and the Higher Education Sprout Project by the Ministry of Education (MOE) in Taiwan.

Disclosure

The authors report no conflicts of interest in this work.

References

1. Mei L, Zhu S, Yin W, et al. Two-dimensional nanomaterials beyond graphene for antibacterial applications: current progress and future perspectives. *Theranostics*. 2020;10(2):757. doi:10.7150/thno.39701
2. Makvandi P, Wang CY, Zare EN, Borzacchiello A, Niu LN, Tay FR. Metal-based nanomaterials in biomedical applications: antimicrobial activity and cytotoxicity aspects. *Adv Funct Mater*. 2020;30:1910021.
3. Roy S, Mondal A, Yadav V, et al. Mechanistic insight into the antibacterial activity of chitosan exfoliated MoS2 nanosheets: membrane damage, metabolic inactivation, and oxidative stress. *ACS Appl Bio Mater*. 2019;2:2738–2755.
4. Singer A, Markoutsa E, Limayem A, Mohapatra S, Mohapatra SS. Nanobiotechnology medical applications: overcoming challenges through innovation. *Eurobiotech J*. 2018;2:146–160.
5. Willyard C. The drug-resistant bacteria that pose the greatest health threats. *Nature News*. 2017;543:15.
6. Teng S-O, Yen M-Y, Ou T-Y, Chen F-L, Yu F-L, Lee W-S. Comparison of pneumonia-and non-pneumonia-related acinetobacter baumannii bacteremia: impact on empiric therapy and antibiotic resistance. *J Microbiol Immunol Infect*. 2015;48:525–530.
7. Ku Y-H, Chuang Y-C, Chen -C-C, et al. Klebsiella pneumoniae isolates from meningitis: epidemiology, virulence and antibiotic resistance. *Sci Rep*. 2017;7:1–10.
8. Jia Q, Song Q, Li P, Huang W. Rejuvenated photodynamic therapy for bacterial infections. *Adv Healthc Mater*. 2019;8:1900608.
9. Zhang Y, Lin C, Lin Q, et al. Cui-bioi/Cu film for enhanced photo-induced charge separation and visible-light antibacterial activity. *Appl Catal B*. 2018;235:238–245.
10. Zhou R, Zhu S, Gong L, Fu Y, Gu Z, Zhao Y. Recent advances of stimuli-responsive systems based on transition metal dichalcogenides for smart cancer therapy. *J Mater Chem B*. 2019;7(16):2588–2607. doi:10.1039/C8TB03240H
11. Chen J, Fan T, Xie Z, et al. Advances in nanomaterials for photodynamic therapy applications: status and challenges. *Biomaterials*. 2020;237:119827.
12. Gong L, Yan L, Zhou R, Xie J, Wu W, Gu Z. Two-dimensional transition metal dichalcogenide nanomaterials for combination cancer therapy. *J Mater Chem B*. 2017;5:1873–1895.
13. Chen T-Y, Kuo T-R, Yougbaré S, Lin L-Y, Xiao C-Y. Novel direct growth of ZIF-67 derived Co3O4 and N-doped carbon composites on carbon cloth as supercapacitor electrodes. *J Colloid Interface Sci*. 2022;608:493–503.
14. Manzeli S, Ovchinnikov D, Pasquier D, Yazyev OV, Kis A. 2D transition metal dichalcogenides. *Nature Rev Mater*. 2017;2:17033.
15. Radisavljevic B, Radenovic A, Brivio J, Giacometti V, Kis A. Single-layer MoS2 transistors. *Nat Nanotech*. 2011;6:147–150.
16. Yin Z, Li H, Li H, et al. Single-layer MoS2 phototransistors. *ACS nano*. 2012;6:74–80.
17. Mak KF, McGill KL, Park J, McEuen PL. The Valley hall effect in MoS2 transistors. *Science*. 2014;344:1489–1492.
18. Li H, Jia X, Zhang Q, Wang X. Metallic transition-metal dichalcogenide nanocatalysts for energy conversion. *Chem*. 2018;4:1510–1537.
19. Gao Y-P, Wu X, Huang K-J, Xing L-L, Zhang Y-Y, Liu L. Two-dimensional transition metal diseleniums for energy storage application: a review of recent developments. *Cryst Eng Comm*. 2017;19:404–418.
20. Zhang X, Teng SY, Loy ACM, How BS, Leong WD, Tao X. Transition metal dichalcogenides for the application of pollution reduction: a review. *Nanomaterials*. 2020;10:1012.
21. Qian X, Shen S, Liu T, Cheng L, Liu Z. Two-dimensional tis 2 nanosheets for in vivo photoacoustic imaging and photothermal cancer therapy. *Nanoscale*. 2015;7:6380–6387.
22. Hao J, Song G, Liu T, et al. In vivo long-term biodistribution, excretion, and toxicology of pegylated transition-metal dichalcogenides ms2 (m= mo, w, ti) nanosheets. *Adv Sci*. 2017;4:1600160.
23. Kuo TR, Chen WT, Liao HJ, et al. Improving hydrogen evolution activity of earth-abundant cobalt-doped iron pyrite catalysts by surface modification with phosphide. *Small*. 2017;13:1603356.
24. Zhu YP, Kuo TR, Li YH, et al. Emerging dynamic structure of electrocatalysts unveiled by in situ X-ray diffraction/absorption spectroscopy. *Energy Environ Sci*. 2021;14:1928–1958.
25. Liang W, Whangbo M-H. Conductivity anisotropy and structural phase transition in covellite CuS. *Solid State Commun*. 1993;85:405–408.
26. Saqib S, Nazeer A, Ali M, et al. Catalytic potential of endophytes facilitates synthesis of biometallic zinc oxide nanoparticles for agricultural application. *Bio Metals*. 2022;35:967–985.
27. Saqib S, Zaman W, Ayaz A, et al. Postharvest disease inhibition in fruit by synthesis and characterization of chitosan iron oxide nanoparticles. *Biocatal Agric Biotechnol*. 2020;28:101729.
28. Saqib S, Zaman W, Ullah F, Majeed I, Ayaz A, Hussain Munis MF. Organometallic assembling of chitosan-iron oxide nanoparticles with their antifungal evaluation against rhizopus oryzae. *Appl Organomet Chem*. 2019;33:e5190.
29. Kappera R, Voiry D, Yalcin SE, et al. Phase-engineered low-resistance contacts for ultrathin MoS2 transistors. *Nat Mater*. 2014;13:1128–1134.
30. Kaur N, Aditya RN, Singh A, Kuo T-R. Biomedical applications for gold nanoclusters: recent developments and future perspectives. *Nanoscale Res Lett*. 2018;13:1–12.
31. Wei M-F, Chen M-W, Chen K-C, et al. Autophagy promotes resistance to photodynamic therapy-induced apoptosis selectively in colorectal cancer stem-like cells. *Autophagy*. 2014;10:1179–1192.

32. Mutalik C, Wang D-Y, Krisnawati DI, Jazidie A, Yougbare S, Kuo T-R. Light-activated heterostructured nanomaterials for antibacterial applications. *Nanomaterials*. 2020;10:643.
33. Liu T, Wang C, Cui W, et al. Combined photothermal and photodynamic therapy delivered by pegylated mos 2 nanosheets. *Nanoscale*. 2014;6:11219–11225.
34. Mukhtar F, Munawar T, Nadeem MS, et al. Highly efficient tri-phase TiO_2-Y_2O_3-V_2O_5 nanocomposite: structural, optical, photocatalyst, and antibacterial studies. *J Nanostructure Chem*. 2022;12:547–564.
35. Mukhtar F, Munawar T, Nadeem MS, et al. Enhanced sunlight-absorption of Fe_2O_3 covered by PANI for the photodegradation of organic pollutants and antimicrobial inactivation. *Adv Powder Technol*. 2022;33:103708.
36. Mukhtar F, Munawar T, Nadeem MS, Rehman MNU, Riaz M, Iqbal F. Dual S-scheme heterojunction ZnO-V_2O_5-WO_3 nanocomposite with enhanced photocatalytic and antimicrobial activity. *Mater Chem Phys*. 2021;263:124372.
37. Naveed Ur Rehman M, Munawar T, Nadeem MS, et al. Facile synthesis and characterization of conducting polymer-metal oxide based core-shell PANI-Pr_2O-NiO-Co_3O_4 nanocomposite: as electrode material for supercapacitor. *Ceram Int*. 2021;47:18497–18509.
38. Munawar T, Mukhtar F, Nadeem MS, et al. Novel direct dual-z-scheme ZnO-Er_2O_3-Nd_2O_3@reduced graphene oxide heterostructured nanocomposite: synthesis, characterization and superior antibacterial and photocatalytic activity. *Mater Chem Phys*. 2020;253:123249.
39. Cheng L, Liu J, Gu X, et al. Pegylated WS2 nanosheets as a multifunctional theranostic agent for in vivo dual-modal ct/photoacoustic imaging guided photothermal therapy. *Adv Mater*. 2014;26:1886–1893.
40. Liu T, Wang C, Gu X, et al. Drug delivery with pegylated MoS2 nano-sheets for combined photothermal and chemotherapy of cancer. *Adv Mater*. 2014;26:3433–3440.
41. Cheng L, Yuan C, Shen S, et al. Bottom-up synthesis of metal-ion-doped WS2 nanoflakes for cancer theranostics. *ACS nano*. 2015;9:11090–11101.
42. Anju S, Mohanan P. Biomedical applications of transition metal dichalcogenides (tmdcs). *Synth Met*. 2021;271:116610.
43. Li Z, Wong SL. Functionalization of 2D transition metal dichalcogenides for biomedical applications. *Mater Sci Engi C*. 2017;70:1095–1106.
44. Dos Santos AF, De Almeida DRQ, Terra LF, Baptista MS, Labriola L. Photodynamic therapy in cancer treatment - an update review. *J Cancer Metastatis Treat*. 2019;5:25.
45. Munawar T, Mukhtar F, Nadeem MS, et al. Fabrication of dual z-scheme TiO_2-WO_3-CeO_2 heterostructured nanocomposite with enhanced photocatalysis, antibacterial, and electrochemical performance. *J Alloys Compd*. 2022;898:162779.
46. Mukhtar F, Munawar T, Nadeem MS, et al. Dual z-scheme core-shell PANI-CeO_2-Fe_2O_3-NiO heterostructured nanocomposite for dyes remediation under sunlight and bacterial disinfection. *Environ Res*. 2022;215:114140.
47. Mukhtar F, Munawar T, Nadeem MS, et al. Enhancement in carrier separation of ZnO-Ho_2O_3-Sm_2O_3 hetrostuctured nanocomposite with rgo and PANI supported direct dual z-scheme for antimicrobial inactivation and sunlight driven photocatalysis. *Adv Powder Technol*. 2021;32:3770–3787.
48. Edelson RL. Light-activated drugs. *Sci Am*. 1988;259:68–75.
49. Josefsen LB, Boyle RW. Photodynamic therapy and the development of metal-based photosensitisers. *Met Based Drugs*. 2008;2008:24.
50. Wang R, Zhang B, Liang Z, et al. Insights into rapid photodynamic inactivation mechanism of staphylococcus aureus via rational design of multifunctional nitrogen-rich carbon-coated bismuth/cobalt nanoparticles. *Appl Catal B*. 2019;241:167–177.
51. Min D, Boff J. Chemistry and reaction of singlet oxygen in foods. *Comprehen Rev Food Sci Food Safe*. 2002;1:58–72.
52. DeRosa MC, Crutchley RJ. Photosensitized singlet oxygen and its applications. *Coord Chem Rev*. 2002;233:351–371.
53. Yougbaré S, Mutalik C, Okoro G, et al. Emerging trends in nanomaterials for antibacterial applications. *Int J Nanomedicine*. 2021;16:5831–5867.
54. Mutalik C, Okoro G, Krisnawati DI, et al. Copper sulfide with morphology-dependent photodynamic and photothermal antibacterial activities. *J Colloid Interface Sci*. 2022;607:1825–1835.
55. Carlson C, Hussain SM, Schrand AM, et al. Unique cellular interaction of silver nanoparticles: size-dependent generation of reactive oxygen species. *J Phys Chem B*. 2008;112:13608–13619.
56. Chernousova S, Epple M. Silver as antibacterial agent: ion, nanoparticle, and metal. *Angew Chem Int Ed*. 2013;52:1636–1653.
57. Kim JS, Kuk E, Yu KN, et al. Antimicrobial effects of silver nanoparticles. *Nanomedicine*. 2007;3:95–101.
58. Mutalik C, Krisnawati DI, Patil SB, et al. Phase-dependent MoS2 nanoflowers for light-driven antibacterial application. *ACS Sustain Chem Eng*. 2021;9:7904–7912.
59. Maitra U, Gupta U, De M, Datta R, Govindaraj A, Rao C. Highly effective visible-light-induced h2 generation by single-layer 1T-MoS2 and a nanocomposite of few-layer 2H-MoS2 with heavily nitrogenated graphene. *Angew Chem Int Ed*. 2013;52:13057–13061.
60. Chen Y, Zhang G, Ji Q, Liu H, Qu J. Triggering of low-valence molybdenum in multiphasic MoS2 for effective reactive oxygen species output in catalytic fenton-like reactions. *ACS Appl Mater Interfaces*. 2019;11:26781–26788.
61. Xu L, Tetreault AR, Pope MA. Chemical insights into the rapid, light-induced auto-oxidation of molybdenum disulfide aqueous dispersions. *Chem Mater*. 2019;32:148–156.
62. Abinaya R, Archana J, Harish S, et al. Ultrathin layered mos 2 nanosheets with rich active sites for enhanced visible light photocatalytic activity. *RSC Adv*. 2018;8:26664–26675.
63. Mutalik C, Hsiao Y-C, Chang Y-H, et al. High uv-vis-nir light-induced antibacterial activity by heterostructured TiO_2-FeS_2 nanocomposites. *Int J Nanomedicine*. 2020;15:8911.
64. Liang Z, Wang H, Zhang K, et al. Oxygen-defective mno2/zif-8 nanorods with enhanced antibacterial activity under solar light. *Chem Eng J*. 2022;428:131349.
65. Liu B, Mu L, Han B, Zhang J, Shi H. Fabrication of TiO2/ag2o heterostructure with enhanced photocatalytic and antibacterial activities under visible light irradiation. *Appl Surf Sci*. 2017;396:1596–1603.
66. Ali T, Ahmed A, Alam U, Uddin I, Tripathi P, Muneer M. Enhanced photocatalytic and antibacterial activities of Ag-doped TiO2 nanoparticles under visible light. *Mater Chem Phys*. 2018;212:325–335.
67. Kim S-G, Dhandole LK, Seo Y-S, et al. Active composite photocatalyst synthesized from inactive rh & sb doped TiO2 nanorods: enhanced degradation of organic pollutants & antibacterial activity under visible light irradiation. *Appl Catal a Gen*. 2018;564:43–55.

68. Kuo T-R, Liao H-J, Chen Y-T, et al. Extended visible to near-infrared harvesting of earth-abundant FeS_2-TiO_2 heterostructures for highly active photocatalytic hydrogen evolution. *Green Chem*. 2018;20:1640–1647.
69. Unnikrishnan B, Gultom IS, Tseng Y-T, Chang H-T, Huang C-C. Controlling morphology evolution of titanium oxide–gold nanourchin for photocatalytic degradation of dyes and photoinactivation of bacteria in the infected wound. *J Colloid Interface Sci*. 2021;598:260–273.
70. Tripathy A, Sen P, Su B, Briscoe WH. Natural and bioinspired nanostructured bactericidal surfaces. *Adv Colloid Interface Sci*. 2017;248:85–104.
71. Anand A, Unnikrishnan B, Wei S-C, Chou CP, Zhang L-Z, Huang -C-C. Graphene oxide and carbon dots as broad-spectrum antimicrobial agents – a minireview. *Nanoscale Horizons*. 2019;4:117–137.
72. Gonçalves I, Abreu AS, Matamá T, et al. Enzymatic synthesis of poly(catechin)-antibiotic conjugates: an antimicrobial approach for indwelling catheters. *Appl Microbiol Biotechnol*. 2015;99:637–651.
73. Ikigai H, Nakae T, Hara Y, Shimamura T. Bactericidal catechins damage the lipid bilayer. *Biochim Biophys Acta*. 1993;1147:132–136.
74. Kajiya K, Hojo H, Suzuki M, Nanjo F, Kumazawa S, Nakayama T. Relationship between antibacterial activity of (+)-catechin derivatives and their interaction with a model membrane. *J Agric Food Chem*. 2004;52:1514–1519.
75. Wu B, Li Y, Su K, et al. The enhanced photocatalytic properties of mno2/g-C3N4 heterostructure for rapid sterilization under visible light. *J Hazard Mater*. 2019;377:227–236.
76. Yu J, Zeng T, Wang H, et al. Oxygen-defective mno2− x rattle-type microspheres mediated singlet oxygen oxidation of organics by peroxymonosulfate activation. *Chem Eng J*. 2020;394:124458.
77. Zhu G, Zhu J, Li W, et al. Tuning the k+ concentration in the tunnels of α-mno2 to increase the content of oxygen vacancy for ozone elimination. *Environ Sci Technol*. 2018;52:8684–8692.
78. Liu G, Zou J, Tang Q, et al. Surface modified ti3c2 mxene nanosheets for tumor targeting photothermal/photodynamic/chemo synergistic therapy. *ACS Appl Mater Interfaces*. 2017;9:40077–40086.
79. Ge J, Lan M, Zhou B, et al. A graphene quantum dot photodynamic therapy agent with high singlet oxygen generation. *Nat Commun*. 2014;5:1–8.
80. Loeb S, Li C, Kim J-H. Solar photothermal disinfection using broadband-light absorbing gold nanoparticles and carbon black. *Environ Sci Technol*. 2018;52:205–213.
81. Pasparakis G. Light-induced generation of singlet oxygen by naked gold nanoparticles and its implications to cancer cell phototherapy. *Small*. 2013;9:4130–4134.
82. Vankayala R, Sagadevan A, Vijayaraghavan P, Kuo CL, Hwang KC. Metal nanoparticles sensitize the formation of singlet oxygen. *Angew Chem Int Ed*. 2011;50:10640–10644.
83. Qu W, Zhao H, Zhang Q, et al. Multifunctional Au/ti3c2 photothermal membrane with antibacterial ability for stable and efficient solar water purification under the full spectrum. *ACS Sustain Chem Eng*. 2021;9:11372–11387.
84. Li Q, Wang W, Feng H, et al. Nir-triggered photocatalytic and photothermal performance for sterilization based on copper sulfide nanoparticles anchored on ti3c2tx mxene. *J Colloid Interface Sci*. 2021;604:810–822.
85. Dai X, Zhao Y, Yu Y, et al. Single continuous near-infrared laser-triggered photodynamic and photothermal ablation of antibiotic-resistant bacteria using effective targeted copper sulfide nanoclusters. *ACS Appl Mater Interfaces*. 2017;9:30470–30479.
86. Li M, Liu X, Tan L, et al. Noninvasive rapid bacteria-killing and acceleration of wound healing through photothermal/photodynamic/copper ion synergistic action of a hybrid hydrogel. *Biomater sci*. 2018;6:2110–2121.
87. Yougbare S, Mutalik C, Krisnawati DI, et al. Nanomaterials for the photothermal killing of bacteria. *Nanomaterials*. 2020;10:1123.
88. Lu T-Y, Chiang C-Y, Fan Y-J, et al. Dual-targeting glycol chitosan/heparin-decorated polypyrrole nanoparticle for augmented photothermal thrombolytic therapy. *ACS Appl Mater Interfaces*. 2021;13:10287–10300.
89. Lu K-Y, Jheng P-R, Lu L-S, Rethi L, Mi F-L, Chuang E-Y. Enhanced anticancer effect of ROS-boosted photothermal therapy by using fucoidan-coated polypyrrole nanoparticles. *Int J Biol Macromol*. 2021;166:98–107.
90. Liao Y-T, Liu C-H, Chin Y, et al. Biocompatible and multifunctional gold nanorods for effective photothermal therapy of oral squamous cell carcinoma. *J Mater Chem B*. 2019;7:4451–4460.
91. Yousefi M, Dadashpour M, Hejazi M, et al. Anti-bacterial activity of graphene oxide as a new weapon nanomaterial to combat multidrug-resistance bacteria. *Mater Sci Engi C*. 2017;74:568–581.
92. Behzadpour N, Sattarahmady N, Akbari N. Antimicrobial photothermal treatment of pseudomonas aeruginosa by a carbon nanoparticles-polypyrrole nanocomposite. *J Biomed Physics Engi*. 2019;9:661.
93. Xu J-W, Yao K, Xu Z-K. Nanomaterials with a photothermal effect for antibacterial activities: an overview. *Nanoscale*. 2019;11:8680–8691.
94. Chen Y, Gao Y, Chen Y, Liu L, Mo A, Peng Q. Nanomaterials-based photothermal therapy and its potentials in antibacterial treatment. *J Controlled Release*. 2020;328:251–262.
95. Zhou Z, Li B, Shen C, et al. Metallic 1T phase enabling MoS2 nanodots as an efficient agent for photoacoustic imaging guided photothermal therapy in the near-infrared-ii window. *Small*. 2020;16:2004173.
96. Zhou Z, Wang X, Zhang H, et al. Activating layered metal oxide nanomaterials via structural engineering as biodegradable nanoagents for photothermal cancer therapy. *Small*. 2021;17:2007486.
97. Lesyuk R, Klein E, Yaremchuk I, Klinke C. Copper sulfide nanosheets with shape-tunable plasmonic properties in the nir region. *Nanoscale*. 2018;10:20640–20651.
98. Wu X, Liu K, Huang Q, et al. Photothermal therapy based on CuS nanoparticles for alleviating arterial restenosis induced by mechanical injury of endovascular treatment. *Front Mater*. 2021;386: 591281.
99. Li C-H, Kuo T-R, Su H-J, et al. Fluorescence-guided probes of aptamer-targeted gold nanoparticles with computed tomography imaging accesses for in vivo tumor resection. *Sci Rep*. 2015;5:15675.
100. Mutalik C, Okoro G, Chou H-L, et al. Phase-dependent 1T/2H-MoS 2 nanosheets for effective photothermal killing of bacteria. *ACS Sustain Chem Eng*. 2022;10(27):8949–8957. doi:10.1021/acssuschemeng.2c02457
101. Yougbaré S, Chou H-L, Yang C-H, et al. Facet-dependent gold nanocrystals for effective photothermal killing of bacteria. *J Hazard Mater*. 2021;407:124617. doi:10.1016/j.jhazmat.2020.124617

102. Patil SB, Chou H-L, Chen Y-M, et al. Enhanced N 2 affinity of 1T-MoS 2 with a unique pseudo-six-membered ring consisting of N–Li–S–Mo–S–Mo for high ambient ammonia electrosynthesis performance. *J Mater Chem A*. 2021;9(2):1230–1239. doi:10.1039/D0TA10696H
103. Kuo T-R, Lee Y-C, Chou H-L, et al. Plasmon-enhanced hydrogen evolution on specific facet of silver nanocrystals. *Chem Mater*. 2019;31(10):3722–3728. doi:10.1021/acs.chemmater.9b00652
104. Ferreira F, Carvalho A, Moura ÍJ, Coutinho J, Ribeiro R. Adsorption of H2, O2, H2O, OH and H on monolayer MoS2. *J Physics Condens Matter*. 2018;30(3):035003. doi:10.1088/1361-648X/aaa03f
105. Centurion F, Merhebi S, Baharfar M, et al. Cell-mediated biointerfacial phenolic assembly for probiotic nano encapsulation.*Adv Funct Mater*. 2022;32(26):2200775. doi:10.1002/adfm.202200775
106. Zhang Y, Jia G, Wang P, et al. Size effect on near infrared photothermal conversion properties of liquid-exfoliated MoS 2 and MoSe 2. *Superlattices Microstruct*. 2017;105:22–27. doi:10.1016/j.spmi.2016.11.058
107. Vecitis CD, Zodrow KR, Kang S, Elimelech M. Electronic-structure-dependent bacterial cytotoxicity of single-walled carbon nanotubes. *ACS nano*. 2010;4(9):5471–5479. doi:10.1021/nn101558x
108. Xu M, Fujita D, Kajiwara S, et al. Contribution of physicochemical characteristics of nano-oxides to cytotoxicity. *Biomaterials*. 2010;31(31):8022–8031. doi:10.1016/j.biomaterials.2010.06.022
109. Shen H, Jiang C, Li W, Wei Q, Ghiladi RA, Wang Q. Synergistic photodynamic and photothermal antibacterial activity of in situ grown bacterial Cellulose/MoS 2 -Chitosan nanocomposite materials with visible light illumination. *ACS Appl Mater Interfaces*. 2021;13(26):31193–31205. doi:10.1021/acsami.1c08178
110. Chen H, He X, Zhou Z, et al. Metallic phase enabling MoS2 nanosheets as an efficient sonosensitizer for photothermal-enhanced sonodynamic antibacterial therapy. *J Nanobiotechnology*. 2022;20:136.
111. Wang Z, Zhang Y-J, Liu M, Peterson A, Hurt RH. Oxidation suppression during hydrothermal phase reversion allows synthesis of monolayer semiconducting mos 2 in stable aqueous suspension. *Nanoscale*. 2017;9:5398–5403.
112. Splendiani A, Sun L, Zhang Y, et al. Emerging photoluminescence in monolayer MoS2. *Nano Lett*. 2010;10:1271–1275.
113. Dai C, Zhang S, Liu Z, Wu R, Chen Y. Two-dimensional graphene augments nanosonosensitized sonocatalytic tumor eradication. *ACS nano*. 2017;11:9467–9480.
114. Wang X, Zhong X, Bai L, et al. Ultrafine titanium monoxide (tio1+ x) nanorods for enhanced sonodynamic therapy. *J Am Chem Soc*. 2020;142:6527–6537.
115. Eda G, Yamaguchi H, Voiry D, Fujita T, Chen M, Chhowalla M. Photoluminescence from chemically exfoliated MoS2. *Nano Lett*. 2011;11:5111–5116.
116. Su K, Tan L, Liu X, et al. Rapid photo-sonotherapy for clinical treatment of bacterial infected bone implants by creating oxygen deficiency using sulfur doping. *ACS nano*. 2020;14:2077–2089.
117. Han H, Xu X, Kan H, et al. Synergistic photodynamic/photothermal bacterial inactivation over heterogeneous quaternized chitosan/silver/cobalt phosphide nanocomposites. *J Colloid Interface Sci*. 2022;616:304–315.
118. Tsai Y-C, Vijayaraghavan P, Chiang W-H, et al. Targeted delivery of functionalized upconversion nanoparticles for externally triggered photothermal/photodynamic therapies of brain glioblastoma. *Theranostics*. 2018;8:1435–1448.
119. Zhu M, Liu X, Tan L, et al. Photo-responsive chitosan/Ag/MoS2 for rapid bacteria-killing. *J Hazard Mater*. 2020;383:121122.
120. Han H, Yang J, Li X, et al. Shining light on transition metal sulfides: new choices as highly efficient antibacterial agents. *Nano Res*. 2021;14:2512–2534.
121. Dai D, Xu H, Ge L, et al. In-situ synthesis of cop co-catalyst decorated zn0.5cd0.5s photocatalysts with enhanced photocatalytic hydrogen production activity under visible light irradiation. *Appl Catal B*. 2017;217:429–436.
122. Liu C, Kong D, Hsu P-C, et al. Rapid water disinfection using vertically aligned MoS2 nanofilms and visible light. *Nat Nanotech*. 2016;11:1098–1104.
123. Yu Z, Jiang L, Liu R, et al. Versatile self-assembled mxene-Au nanocomposites for SERS detection of bacteria, antibacterial and photothermal sterilization. *Chem Eng J*. 2021;426:131914.
124. Rasool K, Helal M, Ali A, Ren CE, Gogotsi Y, Mahmoud KA. Antibacterial activity of ti3c2t x mxene. *ACS Nano*. 2016;10:3674–3684.
125. Wu F, Zheng H, Wang W, et al. Rapid eradication of antibiotic-resistant bacteria and biofilms by mxene and near-infrared light through photothermal ablation. *Sci China Mater*. 2021;64:748–758.
126. Ji J, Zhao L, Shen Y, Liu S, Zhang Y. Covalent stabilization and functionalization of mxene via silylation reactions with improved surface properties. *FlatChem*. 2019;17:100128.
127. Premasiri W, Moir D, Klempner M, Krieger N, Jones G, Ziegler L. Characterization of the surface enhanced Raman scattering (SERS) of bacteria. *J Phys Chem B*. 2005;109:312–320.
128. Li Q, Mahendra S, Lyon DY, et al. Antimicrobial nanomaterials for water disinfection and microbial control: potential applications and implications. *Water Res*. 2008;42:4591–4602.
129. Eaton P, Fernandes JC, Pereira E, Pintado ME, Malcata FX. Atomic force microscopy study of the antibacterial effects of chitosans on Escherichia coli and staphylococcus aureus. *Ultramicroscopy*. 2008;108:1128–1134.
130. Akhavan O, Ghaderi E. Toxicity of graphene and graphene oxide nanowalls against bacteria. *ACS nano*. 2010;4:5731–5736.
131. Zhao Q-L, Fujiwara Y, Kondo T. Mechanism of cell death induction by nitroxide and hyperthermia. *Free Radical Biol Med*. 2006;40:1131–1143.
132. Lin H, Wang X, Yu L, Chen Y, Shi J. Two-dimensional ultrathin mxene ceramic nanosheets for photothermal conversion. *Nano Lett*. 2017;17:384–391.
133. Wang S, Singh AK, Senapati D, Neely A, Yu H, Ray PC. Rapid colorimetric identification and targeted photothermal lysis of salmonella bacteria by using bioconjugated oval-shaped gold nanoparticles. *Chem Eur J*. 2010;16:5600–5606.
134. Rudolph B, Gebendorfer KM, Buchner J, Winter J. Evolution of Escherichia coli for growth at high temperatures. *J Biol Chem*. 2010;285:19029–19034.
135. Dong X, Ye J, Chen Y, Tanziela T, Jiang H, Wang X. Intelligent peptide-nanorods against drug-resistant bacterial infection and promote wound healing by mild-temperature photothermal therapy. *Chem Eng J*. 2022;432:134061.

136. Chen J, Dai T, Yu J, et al. Integration of antimicrobial peptides and gold nanorods for bimodal antibacterial applications. *Biomater Sci*. 2020;8:4447–4457.
137. Xie X, Mao C, Liu X, et al. Tuning the bandgap of photo-sensitive polydopamine/ag3po4/graphene oxide coating for rapid, noninvasive disinfection of implants. *ACS Central Sci*. 2018;4:724–738.
138. Van Aken B. Gene expression changes in plants and microorganisms exposed to nanomaterials. *Curr Opin Biotechnol*. 2015;33:206–219.
139. Wang Z, Fang Y, Zhou X, et al. Embedding ultrasmall Ag nanoclusters in luria-bertani extract via light irradiation for enhanced antibacterial activity. *Nano Res*. 2020;13:203–208.
140. Liu M, He D, Yang T, et al. An efficient antimicrobial depot for infectious site-targeted chemo-photothermal therapy. *J Nanobiotechnology*. 2018;16:1–20.
141. Gao G, Jiang YW, Guo Y, et al. Enzyme-mediated tumor starvation and phototherapy enhance mild-temperature photothermal therapy. *Adv Funct Mater*. 2020;30:1909391.
142. Gao G, Jiang YW, Sun W, et al. Molecular targeting-mediated mild-temperature photothermal therapy with a smart albumin-based nanodrug. *Small*. 2019;15:1900501.
143. Qi X, Huang Y, You S, et al. Engineering robust Ag-decorated polydopamine nano-photothermal platforms to combat bacterial infection and prompt wound healing. *Adv Sci*. 2022;9:2106015.
144. Miao H, Shen R, Zhang W, et al. Near-infrared light triggered silk fibroin scaffold for photothermal therapy and tissue repair of bone tumors. *Adv Funct Mater*. 2021;31:2007188.
145. Huang WC, Ying R, Wang W, et al. A macroporous hydrogel dressing with enhanced antibacterial and anti-inflammatory capabilities for accelerated wound healing. *Adv Funct Mater*. 2020;30:2000644.
146. Liu Y, Xiao Y, Cao Y, Guo Z, Li F, Wang L. Construction of chitosan-based hydrogel incorporated with antimonene nanosheets for rapid capture and elimination of bacteria. *Adv Funct Mater*. 2020;30:2003196.
147. Qiao Y, He J, Chen W, et al. Light-activatable synergistic therapy of drug-resistant bacteria-infected cutaneous chronic wounds and nonhealing keratitis by cupriferous hollow nanoshells. *ACS Nano*. 2020;14:3299–3315.
148. Ran L, Lu B, Qiu H, et al. Erythrocyte membrane-camouflaged nanoworms with on-demand antibiotic release for eradicating biofilms using near-infrared irradiation. *Bioact Mater*. 2021;6:2956–2968.
149. Manivannan K, Cheng C-C, Anbazhagan R, Tsai H-C, Chen J-K. Fabrication of silver seeds and nanoparticle on core-shell Ag@ sio2 nanohybrids for combined photothermal therapy and bioimaging. *J Colloid Interface Sci*. 2019;537:604–614.
150. Gao Y, Li Z, Huang J, Zhao M, Wu J. In situ formation of injectable hydrogels for chronic wound healing. *J Mater Chem B*. 2020;8:8768–8780.
151. Kuo JC, Tan SH, Hsiao YC, et al. Unveiling the antibacterial mechanism of gold nanoclusters via in situ transmission electron microscopy. *ACS Sustain Chem Eng*. 2022;10:464–471.
152. Tan S-H, Yougbaré S, Tao H-Y, Chang -C-C, Kuo T-R. Plasmonic gold nanoisland film for bacterial theranostics. *Nanomaterials*. 2021;11:3139.
153. Yougbaré S, Mutalik C, Chung P-F, et al. Gold nanorod-decorated metallic MoS2 nanosheets for synergistic photothermal and photodynamic antibacterial therapy. *Nanomaterials*. 2021;11:3064.
154. Chang T-K, Cheng T-M, Chu H-L, et al. Metabolic mechanism investigation of antibacterial active cysteine-conjugated gold nanoclusters in escherichia coli. *ACS Sustain Chem Eng*. 2019;7:15479–15486.
155. Tang S, Zheng J. Antibacterial activity of silver nanoparticles: structural effects. *Adv Healthc Mater*. 2018;7:1701503.
156. Mukhtar F, Munawar T, Nadeem MS, et al. Multi metal oxide NiO-Fe_2O_3-CdO nanocomposite-synthesis, photocatalytic and antibacterial properties. *Appl Phys A*. 2020;126:588.
157. Hossain MK, Rubel MHK, Akbar MA, et al. A review on recent applications and future prospects of rare earth oxides in corrosion and thermal barrier coatings, catalysts, tribological, and environmental sectors. *Ceram Int*. 2022;48:32588–32612.
158. Munawar T, Nadeem MS, Mukhtar F, et al. Synthesis, characterization, and antibacterial study of novel Mg0.9Cr0.05M0.05O (m = Co, Ag, Ni) nanocrystals. *Phys B Condens Matter*. 2021;602:412555.
159. Finney LA, O'Halloran TV. Transition metal speciation in the cell: insights from the chemistry of metal ion receptors. *Science*. 2003;300:931–936.
160. Hajipour MJ, Fromm KM, Ashkarran AA, et al. Antibacterial properties of nanoparticles. *Trends Biotechnol*. 2012;30:499–511.
161. Wang L, Hu C, Shao L. The antimicrobial activity of nanoparticles: present situation and prospects for the future. *Int J Nanomedicine*. 2017;12:1227.
162. Slavin YN, Asnis J, Häfeli UO, Bach H. Metal nanoparticles: understanding the mechanisms behind antibacterial activity. *J Nanobiotechnology*. 2017;15:1–20.
163. Sukhanova A, Bozrova S, Sokolov P, Berestovoy M, Karaulov A, Nabiev I. Dependence of nanoparticle toxicity on their physical and chemical properties. *Nanoscale Res Lett*. 2018;13:1–21.
164. Shaikh S, Nazam N, Rizvi SMD, et al. Mechanistic insights into the antimicrobial actions of metallic nanoparticles and their implications for multidrug resistance. *Int J Mol Sci*. 2019;20:2468.
165. Godoy-Gallardo M, Eckhard U, Delgado LM, et al. Antibacterial approaches in tissue engineering using metal ions and nanoparticles: from mechanisms to applications. *Bioact Mater*. 2021;6:4470–4490.
166. Saqib S, Faryad S, Afridi MI, et al. Bimetallic assembled silver nanoparticles impregnated in aspergillus fumigatus extract damage the bacterial membrane surface and release cellular contents. *Coatings*. 2022;12:1505.
167. Tang X, Hu W, Ke X, Zheng Y, Ge Q. Antibacterial and desalting behavior of forward osmosis membranes engineered with metal ions. *Desalination*. 2022;530:115655.
168. Mukherjee M, De S. Antibacterial polymeric membranes: a short review. *Environ Sci*. 2018;4:1078–1104.
169. Armendariz Ontiveros M, Quintero Y, Llanquilef A, et al. Anti-biofouling and desalination properties of thin film composite reverse osmosis membranes modified with copper and iron nanoparticles. *Materials*. 2019;12:2081.
170. Hu W, Chen Y, Dong X, Meng Q-W, Ge Q. Positively charged membranes constructed via complexation for chromium removal through micellar-enhanced forward osmosis. *Chem Eng J*. 2021;420:129837.
171. Li M, Ma Z, Zhu Y, et al. Toward a molecular understanding of the antibacterial mechanism of copper-bearing titanium alloys against staphylococcus aureus. *Adv Healthc Mater*. 2016;5:557–566.

172. Klein TY, Wehling J, Treccani L, Rezwan K. Effective bacterial inactivation and removal of copper by porous ceramics with high surface area. *Environ Sci Technol*. 2013;47:1065–1072.
173. Pallela PNVK, Ummey S, Ruddaraju LK, et al. Antibacterial efficacy of green synthesized α-Fe2O3 nanoparticles using sida cordifolia plant extract. *Heliyon*. 2019;5:e02765.
174. Zheng Z, Guo J, Mao H, Xu Q, Qin J, Yan F. Metal-containing poly(ionic liquid) membranes for antibacterial applications. *ACS Biomater Sci Eng*. 2017;3:922–928.
175. Wintachai P, Paosen S, Yupanqui CT, Voravuthikunchai SP. Silver nanoparticles synthesized with eucalyptus critriodora ethanol leaf extract stimulate antibacterial activity against clinically multidrug-resistant acinetobacter baumannii isolated from pneumonia patients. *Microb Pathog*. 2019;126:245–257.
176. Smani Y, McConnell MJ, Pachón J. Role of fibronectin in the adhesion of acinetobacter baumannii to host cells. *PLoS One*. 2012;7:e33073.
177. Choi CH, Lee JS, Lee YC, Park TI, Lee JC. Acinetobacter baumannii invades epithelial cells and outer membrane protein a mediates interactions with epithelial cells. *BMC Microbiol*. 2008;8:1–11.
178. Lee H-W, Koh Y, Kim J, et al. Capacity of multidrug-resistant clinical isolates of acinetobacter baumannii to form biofilm and adhere to epithelial cell surfaces. *Clin Microbiol Infect*. 2008;14:49–54.
179. Costa GFDM, Tognim MCB, Cardoso CL, Carrara-Marrone FE, Garcia LB. Preliminary evaluation of adherence on abiotic and cellular surfaces of acinetobacter baumannii strains isolated from catheter tips. *Brazilian J Infect Dis*. 2006;10:346–351.
180. Lee JC, Koerten H, Van den Broek P, et al. Adherence of acinetobacter baumannii strains to human bronchial epithelial cells. *Res Microbiol*. 2006;157:360–366.
181. Iwashkiw JA, Seper A, Weber BS, et al. Identification of a general O-linked protein glycosylation system in acinetobacter baumannii and its role in virulence and biofilm formation. *PLoS Pathog*. 2012;8:e1002758.
182. Wan S, Kelly PM, Mahon E, et al. The "sweet" side of the protein Corona: effects of glycosylation on nanoparticle–cell interactions. *ACS nano*. 2015;9:2157–2166.
183. Yameen B, Choi WI, Vilos C, Swami A, Shi J, Farokhzad OC. Insight into nanoparticle cellular uptake and intracellular targeting. *J Controlled Release*. 2014;190:485–499.
184. Mordmuang A, Shankar S, Chethanond U, Voravuthikunchai SP. Effects of rhodomyrtus tomentosa leaf extract on staphylococcal adhesion and invasion in bovine udder epidermal tissue model. *Nutrients*. 2015;7:8503–8517.
185. Mu H, Tang J, Liu Q, Sun C, Wang T, Duan J. Potent antibacterial nanoparticles against biofilm and intracellular bacteria. *Sci Rep*. 2016;6:1–9.
186. Anuj SA, Gajera HP, Hirpara DG, Golakiya BA. Interruption in membrane permeability of drug-resistant staphylococcus aureus with cationic particles of nano-silver. *Eur J Pharma Sci*. 2019;127:208–216.
187. Saptarshi SR, Duschl A, Lopata AL. Interaction of nanoparticles with proteins: relation to bio-reactivity of the nanoparticle. *J Nanobiotechnology*. 2013;11:1–12.
188. Müller A, Wenzel M, Strahl H, et al. Daptomycin inhibits cell envelope synthesis by interfering with fluid membrane microdomains. *Proce Natl Acad Sci*. 2016;113:E7077–E7086.
189. Halder S, Yadav KK, Sarkar R, et al. Alteration of zeta potential and membrane permeability in bacteria: a study with cationic agents. *SpringerPlus*. 2015;4:1–14.
190. Das B, Dash SK, Mandal D, et al. Green synthesized silver nanoparticles destroy multidrug resistant bacteria via reactive oxygen species mediated membrane damage. *Arabian J Chem*. 2017;10:862–876.
191. Chen M, Yang Z, Wu H, Pan X, Xie X, Wu C. Antimicrobial activity and the mechanism of silver nanoparticle thermosensitive gel. *Int J Nanomedicine*. 2011;6:2873.
192. Gould IM, David MZ, Esposito S, et al. New insights into meticillin-resistant staphylococcus aureus (mrsa) pathogenesis, treatment and resistance. *Int J Antimicrob Agents*. 2012;39:96–104.
193. Lopez-Carrizales M, Velasco KI, Castillo C, et al. In vitro synergism of silver nanoparticles with antibiotics as an alternative treatment in multiresistant uropathogens. *Antibiotics*. 2018;7:50.
194. MuKherjee M, BaSu S, Mukherjee SK, MajuMder M. Multidrug-resistance and extended spectrum beta-lactamase production in uropathogenic e. Coli which were isolated from hospitalized patients in Kolkata, India. *J Clin Diagnos Res*. 2013;7:449.
195. Flores-Mireles AL, Walker JN, Caparon M, Hultgren SJ. Urinary tract infections: epidemiology, mechanisms of infection and treatment options. *Nat Rev Microbiol*. 2015;13:269–284.
196. Hwang I-S, Hwang JH, Choi H, Kim K-J, Lee DG. Synergistic effects between silver nanoparticles and antibiotics and the mechanisms involved. *J Med Microbiol*. 2012;61:1719–1726.
197. Odds FC. Synergy, antagonism, and what the chequerboard puts between them. *J Antimicrob Chemother*. 2003;52:1.